The physics of neutron stars

2010 Phys.-Usp. 53 1235

(http://iopscience.iop.org/1063-7869/53/12/R03)

Physics – Uspekhi **53** (12) 1235 – 1256 (2010)

REVIEWS OF TOPICAL PROBLEMS

PACS numbers: **26.60. – c**, 97.60.Gb, 97.60.Jd

IN MEMORY OF VITALY LAZAREVICH GINZBURG

The physics of neutron stars

A Y Potekhin

DOI: 10.3367/UFNe.0180.201012b.1279

Contents

1. Introduction **1235**

2. Basic facts about neutron stars **1236**

2.1 Neutron stars as relativistic objects; 2.2 The biggest enigmas of the neutron star structure; 2.3 The birth, life, and death of a neutron star; 2.4 The formation of neutron star concepts

3. Observational manifestations of neutron stars **1240**

3.1 Cooling neutron stars; 3.2 Pulsars; 3.3 Neutron stars in binary systems

4. The core of a neutral star and supernuclear density matter **1242**

4.1 The outer core; 4.2 The inner core and hyperons; 4.3 Phase transformations and deconfinement; 4.4 Relation to observations

5. Envelopes **1247**

5.1 Inner crust; 5.2 Mantle; 5.3 Outer crust and its melting; 5.4 Ocean; 5.5 Atmosphere

6. Magnetic fields **1248**

6.1 Magnetic field strength and evolution; 6.2 Landau quantization; 6.3 Atoms and ions in magnetic atmospheres; 6.4 Electron heat and charge transfer coefficients

7. Cooling and thermal radiation **1251**

7.1 Cooling stages; 7.2 Thermal structure; 7.3 Cooling curves; 7.4 Effective temperatures; 7.5 Masses and radii

8. Conclusion **1254**

References **1254**

Abstract. Topical problems in the physics of and basic facts about neutron stars are reviewed. The observational manifestations of neutron stars, their core and envelope structure, magnetic fields, thermal evolution, and masses and radii are briefly discussed, along with the underlying microphysics.

1. Introduction

Neutron stars, the most compact stars in the Universe, were given this name because their interior is largely composed of neutrons. A neutron star of the typical mass $M \sim 1-2\,M_\odot$, where $M_\odot = 2 \times 10^{33}$ g is the solar mass, has the radius $R \approx 10-14$ km. The density ρ of the stellar matter is $\sim 10^{15}$ g cm $^{-3}$, or roughly 3 times the typical density of a heavy atomic nucleus (normal nuclear density is $\rho_0 = 2.8 \times 10^{14}$ g cm $^{-3}$). The density ρ in the center of a neutron star may be an order of magnitude higher than ρ_0. Such matter cannot be obtained under laboratory conditions, and its properties and even composition remain to be clarified. There are a variety of theoretical models to describe neutron star matter, but a choice in favor of one of them in the near future will be possible only after the analysis and interpretation of relevant observational data using these models. Neutron stars exhibit a variety of unique properties (that are discussed below) and produce many visible manifestations that can be used to verify theoretical models of extreme states of matter [1]. On the other hand, recent progress in theoretical physics studying matter under extreme conditions creates prerequisites for the construction of correct models of neutron stars and adequate interpretation of their observations.

Neutron stars are not the sole objects in whose depth matter is compressed to high densities inaccessible in laboratory. Other representatives of compact stars are white dwarfs and hypothetical quark stars [2]. While the size of a neutron star largely depends on the balance between gravity force and degenerate neutron pressure, white dwarfs resist gravitational squeezing due to the electron degeneracy pressure, and quark or strange stars resist it due to the pressure of matter composed of quarks not combined into hadrons. Neutron stars are much more compact than white dwarfs. White dwarfs, regarded as a peculiar class of stars since the 1910s, have the mass $M \sim M_\odot$ and the radius $R \sim 10^4$ km comparable to Earth's radius but almost 1000 times greater than the radius of a neutron star [3]. Therefore, the matter density in their interiors is less than one-thousandth of ρ_0. It has been calculated that quark stars

A Y Potekhin Ioffe Physical Technical Institute,
Russian Academy of Sciences
ul. Politekhnicheskaya 26, 194021 St. Petersburg, Russian Federation
Tel. (7-812) 292 71 80. Fax (7-812) 550 48 90
E-mail: palex@astro.ioffe.ru

Received 2 August 2010
Uspekhi Fizicheskikh Nauk **180** (12) 1279 – 1304 (2010)
DOI: 10.3367/UFNr.0180.201012b.1279
Translated by Yu V Morozov; edited by A M Semikhatov

with a mass $M \sim M_\odot$ may be even more compact than neutron stars. However, nobody thus far has seen them and their very existence is questioned.

Vitaly Lazarevich Ginzburg was a pioneer of neutron star theoretical research. He predicted certain important features of these objects before they were discovered by radio astronomers in 1967 and greatly contributed to the interpretation of observational data in the subsequent period. A few of his papers concerning these issues were published in 1964. In Refs [4, 5] (the latter in co-authorship with L M Ozernoi), he described changes in the stellar magnetic field during collapse (catastrophic compression) and obtained the value $B \sim 10^{12}$ G, accurate to an order of magnitude for typical magnetic induction of a neutron star with a mass $M \sim M_\odot$ formed in the collapse. Moreover, Ginzburg derived expressions for the magnetic dipole field and the field uniform at infinity taking account of the space-time curvature near the collapsed star, in accordance with the general theory of relativity. Today, these expressions are widely used to study magnetic neutron stars. In the same work, he predicted the existence of a neutron star magnetosphere in which relativistic charged particles emit electromagnetic waves in the radio to X-ray frequency range, and demonstrated the influence of magnetic pressure and magnetohydrodynamic instability and the possibility of detachment of the current-carrying envelope from the collapsing star [5]. Subsequent theoretical and observational studies confirmed the importance of these problems for the neutron star physics. In a one-and-a-half-page note [6], Ginzburg and Kirzhnits formulated a number of important propositions concerning neutron superfluidity in the interior of neutron stars (apparently independently of the earlier note by Migdal [7]), the formation of Feynman–Onsager vortex lines, a critical superfluidity temperature $T_c \lesssim 10^{10}$ K and its dependence on the density $\rho \sim 10^{13} - 10^{15}$ g cm^{-3}, and the influence of neutron superfluidity on heat capacity and therefore on the thermal evolution of a neutron star. These inferences, fully confirmed in later research, were further developed in review [8], where the author considered, inter alia, the superfluidity of neutrons and the superconductivity of a proton admixture in the neutron fluid in the core of a neutron star. In [9], Ginzburg and Syrovatskii put forward the hypothesis of magnetic bremsstrahlung radiation from the source of X-rays in the Crab Nebula that turned out to be a plerion (a pulsar wind nebula) surrounding the neutron star and of its origin from the envelope stripped off in collapse. Ginzburg and co-workers greatly contributed to the elucidation of the nature of radio pulsars, i.e., cosmic sources of periodic radio pulses. In 1968, they developed the model of oscillating white dwarfs [10, 11] and thereafter the models of rotating neutron stars with strong magnetic fields [12–14]; in parallel, they proposed putative mechanisms of pulsar radiation [15, 16]. A few papers were devoted to the role of pulsars in the generation of cosmic rays [17] and the estimation of the work function needed to eject ions from the pulsar surface into the magnetosphere [18]. In 1971, Ginzburg published a comprehensive review [19] focused on the analysis of theoretical concepts of the neutron star physics and the physical nature of pulsars formulated by that time. The review contained a number of important original ideas, such as the estimation of typical neutron star magnetic fields $B \sim 10^{12}$ G with variations from $B \sim 10^8$ to $B \sim 10^{13} - 10^{15}$ G. These estimates were confirmed by later studies that showed a maximum in the magnetic field distribution of radio pulsars around $B \sim 10^{12}$ G [20]; millisecond pulsars discovered in the 1980s proved to have magnetic fields $B \sim 10^8 - 10^{10}$ G [21] and magnetars (the 1990s) $B \sim 10^{14} - 10^{15}$ G [22]. Many of Ginzburg's other findings found wide application in neutron star research. Suffice it to mention, besides the famous studies on superfluidity and superconductivity, investigations into the distribution of electromagnetic waves in the magnetoactive plasma, summarized in the comprehensive monograph [23].

Neutron stars are still known insufficiently and remain puzzling objects despite their extensive study in many research centers during the last 40 years. The aim of this review, from the perspective of modern astrophysics, is to highlight the main features of neutron stars making them unique cosmic bodies. It does not pretend to be comprehensive, bearing in mind the thousands of publications devoted to neutron stars, and is designed first and foremost to present the author's personal view of the problem. Fundamentals of neutron star physics are expounded in the excellent textbook by Shapiro and Teukolsky [24]. A detailed description of developments in selected branches of neutron star astrophysics can be found in monographs such as [2, 25], and specialized reviews published in *Physics Uspekhi*, among other journals, e.g. [21, 26, 27].

Section 2 contains general information on the physical properties of neutron stars and related physical and astrophysical problems; the history of relevant research is outlined. Section 3 is a concise illustration of the diversity of neutron stars as viewed by a terrestrial observer. The following sections are of a less general character, each being concerned with a specific aspect of astrophysics, the list of which is far from exhaustive. For example, the physics of the pulsar magnetosphere and the mechanisms underlying generation of its radiation are not considered because these issues are dealt with in the voluminous literature (see [14, 27–29]). The same refers to nucleon superfluidity discussed in comprehensive reviews [26, 30]. The list of references is neither exhaustive nor representative. It could not be otherwise, keeping in view the format of the article. The author apologizes to those researchers whose important contributions to the physics of neutron stars are not cited in this publication. A more complete bibliography can be found in monograph [25].

2. Basic facts about neutron stars

2.1 Neutron stars as relativistic objects

Of great importance for neutron stars, unlike ordinary ones, are the effects of the general relativity theory (GR) [31]. The structure of nonrotating stars is described by the relativistic equation of hydrostatic equilibrium for a spherically symmetric body in GR known as the Tolman–Oppenheimer–Volkoff (TOV) equation [32, 33]. It also gives a very good approximation for rotating stars, except those with millisecond rotation periods. The minimal possible period is ~ 0.5 ms, but that observed to date is almost thrice as large, 1.396 ms [34], characteristic of the 'slow rotation regime' in which the effects of rotation can be taken into account in terms of the perturbation theory [25, Ch. 6]. The corrections introduced by the magnetic field are negligibly small for the large-scale structure of a neutron star (at least for $B \lesssim 10^{16}$ G). The effects of the known magnetic fields $B < 10^{15}$ G may be of importance in the star envelopes, as we show in Section 6. Solution of the TOV equation for a given equation of state of

neutron star matter yields a family of stellar structure models, whose parameter is the density ρ_c in the center of the star. The stability condition requiring that $M(\rho_c)$ be an increasing function is satisfied within a certain range of stellar masses and radii; the maximum mass M_{max} allowable by the modern theory is approximately $1.5–2.5M_\odot$, depending on the equation of state being used, while the minimal possible mass of a neutron star is $M_{min} \sim 0.1M_\odot$. The significance of the effects of general relativity for a specific star is determined by the compactness parameter

$$x_g = \frac{r_g}{R}, \quad (1)$$

where

$$r_g = \frac{2GM}{c^2} \approx \frac{2.95M}{M_\odot} \text{ km}$$

is the Schwarzschild gravitational radius, G is the gravitational constant, and c is the speed of light. Acceleration of gravity at the stellar surface is given by

$$g = \frac{GM}{R^2\sqrt{1-x_g}} \approx \frac{1.328 \times 10^{14}}{\sqrt{1-x_g}} \frac{M/M_\odot}{R_6^2} \text{ cm s}^{-2}, \quad (2)$$

where $R_6 \equiv R/(10^6 \text{ cm})$.

The canonical neutron star is traditionally a star with $M = 1.4M_\odot$ and $R = 10$ km ($g = 2.425 \times 10^{14}$ cm s^{-2}). We note that the best and most detailed equations of state available to date predict a slightly lower compactness: $R \approx 12$ km at $M = 1.4M_\odot$ (see Section 4.4). Substituting these estimates in (1) shows that the effects of general relativity for a typical neutron star amount to tens of percent. This has two important corollaries: first, the quantitative theory of neutron stars must be wholly relativistic; second, observations of neutron stars open up unique opportunities for measuring the GR effects and verifying the GR predictions.

The near-surface photon frequency (denoted by ω_0) in a locally inertial reference frame undergoes a redshift to ω_∞ with the distance from the star according to

$$z_g \equiv \frac{\omega_0}{\omega_\infty} - 1 = (1-x_g)^{-1/2} - 1. \quad (3)$$

Therefore, the thermal radiation spectrum of a star with an effective temperature T_{eff} is displaced toward longer wavelengths and corresponds to a lower effective temperature $T_{eff}^\infty = T_{eff}\sqrt{1-x_g}$.

Besides the radius R, determined by the equator length $2\pi R$ in a locally inertial reference frame, the apparent radius for a distant observer $R_\infty = R(1+z_g)$ is frequently introduced. Specifically, for the canonical neutron star model, $R_\infty = 13$ km, and for a more realistic model of the same mass, $R_\infty \sim 15$ km. The radius R of a neutron star decreases as its mass increases, but the growth of z_g with the reduction of the radius and the increase in the mass is responsible for a minimum in the dependence $R_\infty(M)$. It can be shown that the apparent stellar radius cannot be smaller than $R_\infty^{min} = 7.66(M/M_\odot)$ km [25]. The overall visible photon luminosity $L_\gamma^\infty \propto R_\infty^2 (T_{eff}^\infty)^4$ is related to the luminosity in the stellar reference frame as $L_\gamma^\infty = (1-x_g)L_\gamma$. The expressions for R_∞ and L_γ^∞ are in excellent agreement with the notion of light bending and time dilation in the vicinity of a massive body. The bending of a light beam enables a distant observer to 'look behind' the stellar horizon. For example, the observer can simultaneously see both polar caps of a star having a dipole magnetic field at a proper dipole inclination angle to the line of sight. This effect actually occurs during observation of pulsars. Naturally, such effects must be taken into account when comparing theoretical models and observations.

According to GR, a rotating star having a shape other than the ellipsoid of revolution must emit gravitational waves. Shape distortions may be caused by star oscillations and other factors. It has been speculated [35] that gravitational waves emitted by rapidly rotating neutron stars can be recorded by modern gravitational antennas. However, these antennas appear more suitable for recording gravitational waves from merging neutron stars [36, 37].

While gravitational waves have not yet been detected by ground-based antennas, they have already been registered in observations of 'space antennas,' i.e., double neutron stars. Two stars orbiting a common center of mass are known to emit gravitational waves. The first pulsar rotating in an orbit together with another neutron star was discovered by Hulse and Taylor in 1974 (Nobel Prize of 1993). It remained the sole known object of this kind for over 20 years. At least 9 such systems have been described to date. The most remarkable of them is the double pulsar system J0737-3039, a binary in which both neutron stars are seen as radio pulsars [21, 38].

The known binary systems of neutron stars have compact orbits and short periods of revolution. The orbital period of the Hulse–Taylor pulsar is less than 8 hours, and the large semiaxis of the orbit is about two million kilometers, or almost two orders of magnitude smaller than the distance between the Sun and Earth. Gravitational radiation is so strong that the loss of energy it carries away results in a significant decrease in both the orbit size and the orbital period. The measured decrease in the orbital period of the Hulse–Taylor pulsar is consistent with that predicted by GR (within a measurement error of a few tenths of a percent).

Another effect of general relativity is the periastron shift or relativistic precession of the orbit that is orders of magnitude greater than Mercury's perihelion shift (in fact, those 7.5% of the latter shift of 0.43″ per year that cannot be accounted for by the influence of other objects of the Solar system are explained in the GR framework). The relativistic periastron shift for the Hulse–Taylor pulsar and the double pulsar is 4.22° per year and 16.9° per year, respectively.

The third measured effect is geodesic precession of a rotating body that moves in an orbit, a precession analogous to the spin–orbital interaction in atomic physics. The measurement of geodesic precession made it possible to reconstruct the time dependence of the direction of the Hulse–Taylor pulsar magnetic axis. It turned out that its directivity pattern would no longer intersect the line of sight of an Earth-based observer around 2025, and the pulsar would become invisible for two centuries [39, 40]. Probably, it will be possible to see its companion star.

The double pulsar proved an even better laboratory than the Hulse–Taylor pulsar for the verification of the effects of general relativity. First, registration of radio pulses from both neutron stars of the binary system allows directly measuring the radial velocities from the Doppler shift and geodesic precession of either star from the altered pulse shape. Second, the line of sight of a terrestrial observer lies virtually in the plane of the double pulsar orbit (at the inclination to the normal $\approx 89°$). This for the first time permitted reliably

measuring the so-called Shapiro delay parameters (two parameters characterizing the time delay of an electromagnetic wave passing a star.[1] Five of the seven independent post-Kepler parameters characterizing the effects of general relativity were measured for the double pulsar. Any two of them uniquely define masses of both pulsars M_A and M_B, while the measurement of the remaining ones may be regarded as verification of GR, which brilliantly passed this test; any two of the measured parameters gave the same values $M_A = 1.337 M_\odot$ and $M_B = 1.249 M_\odot$ up to a measurement error less than $0.001 M_\odot$ [38].

One more unique relativistic object discovered in 2005 is the pulsar PSR J1903 + 0327, having the self-rotation period 2.15 ms and moving in an inclined highly elliptical orbit (eccentricity $e = 0.44$, inclination 78°) with the period 95 days in a pair with a main-sequence star (an ordinary star of a mass $M \approx M_\odot$ identified in the infrared spectral range [41]). Observations with the Arecibo radio telescope yielded three post-Kepler parameters: both Shapiro delay parameters and the orbital precession. The estimate $M = 1.67 \pm 0.01 M_\odot$ was obtained for the pulsar mass under the assumption that the orbital precession is due to the effects of GR alone [42]. It is the largest mass of neutron stars measured thus far. We note, however, that the influence of nonrelativistic effects, such as tides at the companion star caused by gravitational attraction of the pulsar, on the orbital precession cannot be totally excluded. With this uncertainty, a more conservative estimate is $M = 1.67 \pm 0.11 M_\odot$ [42] (see the Note added in proof).

2.2 The biggest enigmas of the neutron star structure

Two main qualitatively different regions, the core and the envelope, are distinguished in a neutron star. The core is in turn subdivided into the outer and inner core, and the envelope into the solid crust and the liquid ocean. Such a division into four essentially different regions was proposed in the review by Ginzburg dated 1971 [19], even if he did not use the above terms (Fig. 1). The outer core of a neutron star is usually several kilometers wide and its matter density is $0.5\rho_0 \lesssim \rho \lesssim 2\rho_0$. This matter, accounting for the largest fraction of the stellar mass, has well-known qualitative characteristics (see [25, Ch. 5, 6]). It is a neutron superfluid with an admixture of the superconducting proton component (see Fig. 1), electrons, and μ^--mesons (muon), all these constituents being strongly degenerate. The inner core occupies the central part with $\rho \gtrsim 2\rho_0$ and with a radius up to several kilometers, and is inherent in rather massive neutron stars ($M \gtrsim 1.4 - 1.5 M_\odot$), while its density in smaller-mass neutron stars is below $2\rho_0$. Neither the composition nor the properties of matter in the inner core are known because the results of their calculation strongly depend on the theoretical description of collective fundamental interactions. From this standpoint, studies of neutron stars are important not only for astrophysics but also for nuclear and elementary particle physics. The available theoretical models presume the following hypothetical options:

1) hyperonization of matter — the appearance of various hyperons (first and foremost, Λ and Σ^- hyperons);

2) pion condensation — formation of a Bose condensate from collective interactions with the properties of π mesons;

[1] We note that the proximity of the orbit plane to the line of sight allowed observing modulation of pulsed emission from one pulsar passing through the atmosphere of the other; this observation provided additional information on their magnetic fields and magnetospheres.

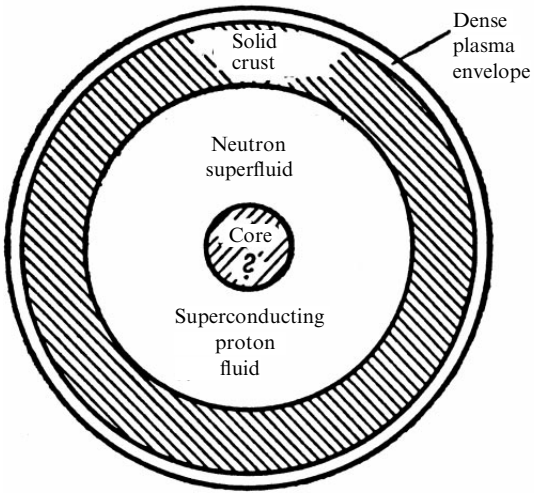

Figure 1. Schematic of the neutron star structure (from Ref. [19] by V L Ginzburg).

3) kaon condensation — formation of a similar condensate from K mesons;

4) deconfinement — phase transition to quark matter.

The last three variants, unlike the first one, are not feasible for all modern theoretical models of matter with supernuclear density; therefore, they are frequently called exotic [25, Ch. 7].

According to current concepts, the core of a neutron star contains superfluid baryonic matter. Superfluidity reduces the heat capacity of this matter and the neutrino reaction rate. However, superfluidity may be responsible for an additional neutrino emission due to Cooper pairing of nucleons at a certain cooling stage in those parts of the star where the temperature decreases below critical values. These effects and their influence on the cooling rate of a neutron star are reviewed in [26].

The envelope consists of more ordinary matter containing isolated atomic nuclei. Nevertheless, this matter also occurs under extreme (from the standpoint of terrestrial physics) conditions that cannot be reproduced in laboratory. This makes such matter a very interesting subject of plasma physics research [1]. Equally important is the fact that an adequate theoretical description of stellar envelopes is indispensable for the correct interpretation of characteristics of the electromagnetic radiation coming from the star, i.e., for the study of its core by means of comparison of theoretical models and astronomical observations.

2.3 The birth, life, and death of a neutron star

A neutron star is a possible end product of a main-sequence star ('normal' star) [3]. Neutron stars are believed to be formed in type-II supernova explosions [43–47]. An explosion occurs after a precursor to a supernova has burned out its nuclear 'fuel': first hydrogen, then helium produced from hydrogen, and finally heavier chemical elements, including oxygen and magnesium. The end product of subsequent nuclear transformations is isotopes of iron-group elements accumulated in the center of the star. The pressure of the electron Fermi gas is the sole factor that prevents collapse of such an iron–nickel core to its center under the force of gravity. But as soon as a few days after oxygen burnoff, the mass of the iron core increases above the Chandrasekhar limit equal to $1.44 M_\odot$, which is the maximum mass whose gravitational compression is still counteracted by the pres-

sure of degenerate electrons. Then gravitational collapse, i.e., a catastrophic breakdown of the stellar core, occurs. It is accompanied by liberation of an enormous gravitational energy ($\gtrsim 10^{53}$ erg) and a shockwave that strips off the outer envelopes of the giant star at a speed amounting to 10% of the speed of light, while the inner part of the star continues to contract at approximately the same rate. The atomic nuclei fuse into a single giant nucleus. If its mass surpasses the Oppenheimer–Volkoff limit, i.e., the maximum mass that the pressure of degenerate neutrons and other hadrons is able to support against gravitational compression ($\approx 2-3M_\odot$ according to modern theoretical models), the compression cannot be stopped and the star collapses to form a black hole. It is believed that the collapse resulting in a black hole may be responsible for the flare from a hypernova hundreds of times brighter than a supernova; it may be a source of mysterious gamma-ray bursts coming from remote galaxies [48, 49]. If the mass remains below the Oppenheimer–Volkoff limit, a neutron star is born whose gravitational squeezing is prevented by the pressure of nuclear matter. In this case, about 1% of the released energy transforms into the kinetic energy of the envelopes flying apart, which later give rise to a nebula (a remnant of the supernova), and only 0.1% ($\sim 10^{49}$ erg) into electromagnetic radiation, which nevertheless may overshine the luminosity of the entire galaxy and is seen as a supernova.

Not every star completes its evolution as a supernova (not to mention a hypernova); only massive stars with $M \gtrsim 8M_\odot$ are destined to have such a fate. A less massive star at the end of its lifetime goes through a giant phase, gradually throwing off the outer envelopes, and its central part shrinks into a white dwarf.

A newborn neutron star has the temperature above $10^{10}-10^{11}$ K; thereafter, it cools down (rather fast initially, but slower and slower afterwards), releasing the energy in the form of neutrino emission from its depth and electromagnetic radiation from the surface. But the evolution of a neutron star is not reduced to cooling alone. Many neutron stars have strong magnetic fields that also evolve through changes in strength and configuration. A rotating neutron star having a strong magnetic field is surrounded by an extended plasma magnetosphere formed due to the knockout of charged particles from the surface by the rotation-induced electric field, thermal emission, and the birth of electron–positron pairs upon collisions of charged particles of the magnetosphere with one another and with photons. Given a sufficiently fast rotation of a star, its magnetosphere undergoes collective acceleration of the constituent particles in the parts where plasma density is too low to screen the strong electric field induced by rotation. Such processes generate a coherent directed radio-frequency emission due to which the neutron star can be seen as a radio pulsar if it rotates such that its directivity pattern intersects observer's line of sight. The rotational energy is gradually depleted and the particles born in the magnetosphere have a charge whose sign is such that the induced electric field makes them propagate toward the star; they accelerate along the magnetic field lines, hit the star surface near its magnetic poles, and heat these regions. A similar process of heating magnetic poles occurs in the case of accretion (infall) of matter onto a star, e.g., as it passes through dense interstellar clouds or as the matter outflows from the companion star in a binary system. The hot polar caps emit much more intense X-rays than the remaining surface; as a result, such neutron stars look like X-ray pulsars. Pulsed X-ray radiation is also observed from thermonuclear explosions of accreted matter at the surface of a rotating neutron star (see, e.g., [50]).

Starquakes may occur as a result of cooling, changes in the magnetic field, or a slowdown of rotation; they are associated with variations of the crustal shape, phase transformations in the core, and interaction between the normal and superfluid components of the core and the crust [51–56]. Starquakes are accompanied by liberation of the thermal energy and sharp changes in the character of rotation [57]. Moreover, the matter falling onto the star during accretion undergoes nuclear transformations at the surface and, due to its weight, causes additional transformations in the depth of the envelope that alter the nuclear composition and liberate energy [58–60]. In other words, neutron stars not only cool down but also are heated from the inside.

A single neutron star eventually exhausts its supply of thermal and magnetic energy and fades away. A star has more promising prospects for the future if it is a member of a binary system. For example, if the companion star overfills its Roche lobe (the region in which matter is gravitationally coupled to the companion), this matter accretes onto the neutron star so intensely as to make it a bright source of X-ray radiation by virtue of the released gravitational and thermonuclear energy. In this case, the inflowing matter forms an accretion disk around the neutron star, which also emits X-ray radiation, and this luminosity changes with time, e.g., as a result of disk precession or variations of the accretion rate. The character of accretion strongly depends on the neutron star magnetization and the rotation period [61]. If the mass of the accreted matter surpasses a critical threshold, the neutron star collapses into a black hole.

If the companion of a neutron star is a compact object, then the radius of their mutual orbit may be small enough to enable gravitational waves emitted by such a system to appreciably influence its evolution. The orbital radius of the compact binary system decreases as gravitational radiation continues until the two companions merge together, giving rise to a black hole with the release of enormous gravitational energy comparable to the stellar rest energy $Mc^2 \sim 10^{54}$ erg in the form of neutrino and gravitational radiation (this will be the case with the Hulse–Taylor pulsar and the binary pulsar in some 300 and 85 million years, respectively).

It may be argued that rotation, accretion, and the magnetic field are the three principal driving forces of the evolution of a neutron star, responsible for its observational manifestations.

2.4 The formation of neutron star concepts

Baade and Zwicky [62] theoretically predicted neutron stars as a probable result of supernova explosions less than 2 years after the discovery of the neutron [63]. They also put forward the hypothesis (now universally accepted) that supernovae are important sources of galactic cosmic rays and coined the term 'supernova' itself to differentiate between these unusually bright objects formed in a gravitational collapse giving rise to a neutron star from more numerous nova stars originating, as is known today, from thermonuclear burning of the accreted matter at the surface of white dwarfs. The popular belief based on Rosenfeld's memoirs [64] that Landau predicted neutron stars in 1932 [24] is ungrounded because the meeting of Landau with N Bohr and L Rosenfeld occurred in 1931, before the discovery of neutrons. Nevertheless, it is true that Landau already foresaw the existence of neutron

stars at that time and suggested a hypothesis according to which stars with a mass greater than $1.5M_\odot$ have a region in their interior where "the density of matter becomes so great that atomic nuclei come in close contact, forming one gigantic nucleus" [65].

Not a single neutron star was observed for 43 years after Baade and Zwicky's prediction. But theorists continued to work. In 1938, Zwicky [66] calculated the maximum binding energy of a neutron star and the gravitational red shift of photons emitted from its surface. A few months later, Tolman [32] and Oppenheimer and Volkoff [33] derived the aforementioned TOV equation; moreover, the latter authors computed the limit mass of a neutron star, $M_{\max}$, although it proved underestimated because they ignored baryon–baryon interactions. Equations of state of nuclear matter began to be extensively studied in the 1950s. In 1959, Cameron [67] obtained the first realistic estimate $M_{\max} \approx 2M_\odot$. He was the first to show that the core of a neutron star may contain hyperons. In the same year, Migdal [7], based on the postulate of superfluidity in atomic nuclei proposed by A Bohr, Mottelson, and Pines [68], predicted superfluidity of the neutron star matter. In 1960, Ambartsumyan and Saakyan [69] derived the equation of state of superdense matter by taking electrons, muons, and all hadrons known at that time into consideration. They hypothesized that the core of a neutron star consists of two components, the outer composed of nucleons and the inner containing hyperons. The following year, Zel'dovich [70] derived an extremely stiff equation of state of a neutron star in which the speed of sound tends to the speed of light as the density increases. Finally, in the 1960s, the first estimates of neutrino emission from the interior of a neutron star [71, 72] and its cooling [72–76] were reported; in addition, the presence of a strong magnetic field was predicted [4, 5] and the deceleration of rotation of a magnetized neutron star due to magnetodipole radiation was calculated [77].

The first simplest models of neutron star cooling already demonstrated that the surface temperature of a typical neutron star might be as high as hundreds of thousands or millions of degrees, meaning that the star emits thermal radiation largely in the form of soft X-rays unable to penetrate Earth's atmosphere. The progress in astronautics and the advent of X-ray astronomy in the early 1960s [78] gave hope that such radiation would be detected in outer space. However, it took almost 30 years to reliably identify thermal X-ray components in the spectra of neutron stars by the X-ray telescope on board the ROSAT satellite, witch produced images with a resolution of a few angular seconds [79].

Other means were proposed to search for neutron stars. Zel'dovich and Guseinov [80] suggested that they could be detected in binary systems with optical stars from the Doppler shifts of optical spectral lines. Kardashev [81] and Pacini [77] put forward the correct hypothesis that the rotational energy of a neutron star was transferred via the magnetic field to the surrounding nebula formed in the collapse at stellar birth. These authors regarded the Crab Nebula as such a candidate object. However, neutron stars unexpectedly manifested themselves as radio pulsars.

As is known, the first pulsar was discovered by radio astronomers at Cambridge in 1967 [82] (a retrospective study of the archives of the Cambridge group gave evidence of radio pulses from pulsars dating back to 1962–1965 [83]). Antony Hewish, who headed the research team, was awarded the Nobel Prize in physics in 1974. An adequate explanation of these observations soon after their publication was proposed by Gold in the paper entitled "Rotating Neutron Stars as the Origin of the Pulsating Radio Sources" [84]. It is less widely known that Shklovsky [85] arrived at the conclusion, based on analysis of X-ray and optical observations, that radiation from Scorpio X-1 (the first X-ray source discovered outside the Solar System [78]) originated from the accretion of matter onto a neutron star from its companion. The validity of this conclusion was recognized later [86], but it was received with skepticism at the time [87].

The discovery of pulsars gave powerful impetus to the development of theoretical and observational studies of neutron stars. With over one thousand publications devoted to these celestial bodies appearing annually, a new class of astronomical objects containing neutron stars is discovered once every few years. For example, X-ray pulsars were described in 1971, bursters (sources of X-ray bursts) in 1975, soft gamma repeaters (SGRs) in 1979, millisecond pulsars in 1982, radio-silent neutron stars in 1996, anomalous X-ray pulsars (AXPs) in 1998, and rapid (rotating) radio transients (RRATs) in 2006. Clearly, it is impossible to cover all these developments in a single review. We try instead to depict the current situation in certain important branches of the theory, although we start with observable manifestations of neutron stars.

3. Observational manifestations of neutron stars

Neutron stars emit light over the entire electromagnetic spectrum. Just as 40 years ago, most of them (about 1900 as of 2010 [20]) are seen as radio pulsars. Some 150 of the known neutron stars are members of binary systems with accretion and manifest themselves largely in the form of X-ray radiation from the accretion disk or flares produced by explosive thermonuclear burning in the star outer layers. Certain such systems make up X-ray transients in which periods of active accretion (usually as long as several days or weeks) alternate with longer periods of quiescence (months or sometimes years) during which X-ray radiation from the hot star surface is recorded. In addition, over one hundred isolated neutron stars are known to emit X-ray radiation.

3.1 Cooling neutron stars

A large part of emission from isolated neutron stars and X-ray transients in quiescence appears to originate at their surface. To interpret this radiation, it is very important to know the properties of envelopes contributing to the spectrum formation. Conversely, comparison of predictions and observations may be used to deduce these properties and to verify theoretical models of dense magnetized plasma. Moreover, investigating the properties of the envelopes provide knowledge of the parameters of a star as a whole and of the observational constraints on such models.

For each theoretical model of neutron stars, a cooling curve describes the dependence of the overall photon luminosity L_γ^∞ in the frame of a distant observer on time t elapsed after the birth of the star (see [88] and the references therein).

There are not many neutron stars in whose spectrum the cooling-related thermal component can be distinguished from the emission produced by processes other than surface heating, e.g., those proceeding in the pulsar magnetosphere, pulsar nebula, and accretion disk. Fortunately, there are exceptions [89], such as relatively young ($t \lesssim 10^5$ years)

pulsars J1119-6127, B1706-44, and Vela, whose spectra are readily divisible into thermal and nonthermal components, and medium-aged ($t \sim 10^6$ years) B0656 + 14, B1055-52, and Geminga pulsars. The spectra of the last three objects, known as the 'three musketeers' [79, 89] are fairly well described by the three-component model (power-law spectrum of magnetospheric origin, thermal spectrum of the hot polar caps, and thermal spectrum of the remaining surface). Even more important is the discovery of radio-silent neutron stars [90] with purely thermal spectra. These are central compact objects (CCOs) in supernova remnants [91] and X-ray dim isolated neutron stars (XDINSs) [92]. It was shown that CCOs may have magnetic fields $B \sim 10^{10} - 10^{11}$ G (slightly weaker than in the majority of normal pulsars but stronger than in millisecond pulsars); XDINSs have magnetic fields $B \gtrsim 10^{13}$ G (slightly stronger than usual ones) [22]. During the last 10 years, seven XDINSs are known, called the 'Magnificent Seven' by astrophysicists [89, 92, 94]. Incidentally, the known CCOs also number seven, but there are three more candidate objects to be included on this list [93]. The spectra of at least five radio-quiet neutron stars exhibit wide absorption lines for which no fully satisfactory theoretical explanation has yet been proposed. Certain authors hypothesize that they can be attributed to ionic cyclotron harmonics in a strong magnetic field, but rigorous quantum mechanical calculations [95, 96] show that such harmonics in neutron star atmospheres are too weak to be observed.

Besides cooling processes, heating processes of different natures occur in neutron stars. Sometimes they compete with the heat delivered to the stellar surface from the core and must be taken into consideration. Such stars include:

— old neutron stars ($t \gtrsim 10^6$ years) for which the cooling curves (disregarding heating) go down to the low temperature region ($T_{\rm eff} \lesssim 10^5$ K),

— magnetars (relatively young ($t \lesssim 10^4$ years) neutron stars with superstrong ($B \gtrsim 10^{14}$ G) magnetic fields manifested as AXP and SGR [22, 94]). The strong X-ray luminosity of magnetars cannot be explained by 'the standard cooling curve' [88]. Thompson [97] suggested that it should be ascribed to heating due to dissipation of a superstrong magnetic field. Recent studies [98–100] have supported this suggestion.

The discussion of neutron star cooling is to be continued in Section 7. For now, we emphasize that the processes of cooling, heating, and heat transfer turn the surface of a neutron star into a source of thermal radiation with the spectral maximum in the soft X-ray region.

3.2 Pulsars

Pulsed radiation related to the proper rotation of neutron stars contains important additional information [24, 28, 101]. For example, simultaneous measurement of emission at several radio frequencies allows determining the degree of dispersion from the phase shift, which in turn permits roughly estimating the distance to a pulsar. Measurements of the pulsation amplitude of the thermal component in the spectrum characterize the nonuniform temperature distribution over the surface. The period of pulsations P and its time derivative $\dot{P}$ for isolated (nonaccreting) pulsars give an idea of the star magnetic field (of its dipole constituent, to be precise) and age:

$$B \sim 10^{19.5}\sqrt{\frac{\dot{P}P}{1\,\mathrm{c}}}\,\mathrm{G}, \quad t \sim t_{\rm PSR} \equiv \frac{0.5P}{\dot{P}}\,, \tag{4}$$

where $t_{\rm PSR}$ is the so-called characteristic age of the pulsar. Such estimate makes no sense for accreting pulsars because their period of rotation may depend on the interaction between the magnetic field and the accretion disk. For example, the rotation can be accelerated by virtue of the transfer of angular momentum from matter falling onto the pulsar; then $\dot{P} < 0$.

We note that the age of a neutron star can be deduced from the age of the remnant of the supernova hosting this star. As a rule, the age of the remnant is inferred with an error $\sim 10\%$ from the rate at which the envelopes fly apart from each other. Certainly, the remnant itself must be accessible to observation, which is rarely the case (as a rule, only at $t \lesssim 10^4$ years). When both the characteristic age and the age of the remnant are known, they are consistent with each other to the order of magnitude, but their numerical difference may be as great as 2–3-fold. This means that none of the age estimation methods is entirely reliable. The exceptions are 5 supernovae whose flares are documented in historical chronicles [102].

Simultaneous measurement of the age and magnetic field permits imposing bounds on the decay rate of the stellar magnetic field. The relevant theoretical estimates are significantly different, depending on the field configuration inside the crust and the core, which in turn depends on the model and on the hypothesis regarding the nature of the field; they also depend on the electric conductivity included in a given model, which is in turn a function of the poorly known chemical composition of the envelopes, the microscopic structure of the crust, the content of admixtures, and the defects of the crystal lattice.

X-ray radiation from pulsars, similarly to radio emission, carries important information. Generally speaking, the X-ray spectrum of pulsars contains both thermal and nonthermal components. The latter is produced in the magnetosphere either by synchrotron radiation or inverse Compton scattering of charged particles accelerated to relativistic energies by magnetospheric electromagnetic fields. This component is usually described by a power-law spectrum. The thermal component is divided into 'hard' and 'soft' constituents. The former is supposed to be a result of radiation from the polar caps heated to millions of degrees, where the magnetic field does not substantially deviate from the normal to the surface. In the dipole field model, the radius of these regions is estimated as

$$R_{\rm cap} \approx \left(\frac{2\pi R^3}{cP}\right)^{1/2} \approx 0.145 R_6^{3/2}\left(\frac{P}{1\,\mathrm{s}}\right)^{-1/2}\,\mathrm{km}\,. \tag{5}$$

The soft constituent corresponds to radiation from the remaining, cooler surface that may be due to the heat coming up from the stellar core or inner crust.

3.2.1 Normal pulsars. Normal pulsars are isolated pulsars with periods from tens of milliseconds to several seconds. Their characteristic magnetic field given by formula (4) varies from a few gigagauss to 10^{14} G (typically, $B \sim 10^{11} - 10^{13}$ G) and the characteristic age is from several centuries to 10^{10} (typically $t_{\rm PSR} \sim 10^5 - 10^8$) years [20]. The X-ray spectrum of thermal radiation from certain normal pulsars has been measured, which allows the cooling theory methods to be applied to their study. Unlike the case of neutron stars lacking pulsation, the estimates of $t_{\rm PSR}$ and B make the class of thermal structure models more definite and thereby restrict the scattering of possible cooling curves.

3.2.2 Millisecond pulsars. Millisecond pulsars have magnetic fields $B \sim 10^8 - 10^{10}$ G and are from tens of millions to hundreds of billions of years old (typical values $t_{\rm PSR} \sim 10^9 - 10^{10}$ years) except PSR J0537-6910, having an abnormally high $\dot{P}$ [20]. The relatively weak magnetic field and the short period of millisecond pulsars may result from the pulsar having passed through the stage of accretion in the course of its evolution, which reduced the magnetic field and increased the angular momentum due to the interaction between the accreting matter and the magnetic field [21, 61]. Certain isolated millisecond pulsars emitting in the X-ray range show a thermal constituent in their spectra produced by radiation from the hot polar caps [103]. It is convenient to write formula (5) for millisecond pulsars in the form $R_{\rm cap} \approx R_6^{3/2}\,(P/21\ {\rm ms})^{-1/2}$ km; this means that the hot region covers a large surface area of the pulsar.

3.2.3 Anomalous X-ray pulsars (AXPs). Many neutron stars manifest themselves through pulsed radiation in the X-ray part of the spectrum. They are referred to as X-ray pulsars. Some of them are located in binary stellar systems. Evidently, such X-ray transients include radio pulsars emitting thermal radiation from the hot polar caps.

Unlike these 'normal' X-ray pulsars, AXPs have an unusually long period, $P \approx 6 - 12$ s, and high X-ray luminosity $\sim 10^{33} - 10^{35}$ erg s^{-1}; they are isolated objects [22, 104]. Their magnetic fields and characteristic ages calculated from (4) suggest that these objects may be magnetars. An alternative explanation of their properties is based on the assumption that they are neutron stars with 'normal' magnetic fields $B \sim 10^{12}$ G that slowly accrete matter from the disk remaining after the supernova explosion [105]. In other words, the nature of these objects remains obscure.

3.3 Neutron stars in binary systems

A neutron star in a binary system is paired with another neutron star, a white dwarf, or an ordinary (nondegenerate) star. Binary systems containing a neutron star and a companion black hole are not known. Measuring the parameters of the binary orbit provides additional characteristics of the neutron star, e.g., its mass.

The infall of matter onto a neutron star is accompanied by the liberation of energy, which turns the system into a source of bright X-ray radiation. Such systems are categorized into markedly different subclasses: low-mass X-ray binary systems with a dwarf (either white or red) of mass $\lesssim 2M_\odot$ as the companion, and relatively short-lived massive systems in which the mass of the companion star is several or tens of times greater than $M_\odot$ and accretion of matter onto the neutron star is extremely intense.

X-ray binaries may be sources of regular (periodic) and irregular radiation, and are subdivided into permanent and temporary (transient). Emission from some of them is modulated by the neutron star rotation, others are sources of quasiperiodic oscillations (QPOs), bursters (neutron stars whose surface from time to time undergoes explosive thermonuclear burning of the accreted matter), and so on.

The QPOs first observed in 1985 [106] occur in X-ray binary systems containing compact objects, such as neutron stars (typically within low-massive X-ray binaries), white dwarfs, and black holes. There are a variety of hypotheses regarding the nature of such oscillations [107–109]. They seem to originate in the accretion disk. According to some hypotheses, they are related to the Kepler frequency of the innermost stable orbit permitted by GR, a resonance in the disk, or a combination of these frequencies with the rotation frequency of the compact object. Given that one of these hypotheses is true, the quasiperiodic oscillations in low-massive X-ray binary systems may become a tool for determining the parameters of neutron stars.

X-ray luminosity of type-I flares in bursters may reach the Eddington limit $L_{\rm Edd} \approx 1.3 \times 10^{38} (M/M_\odot)$ erg s^{-1} at which the radiation pressure on the plasma due to the Thomson scattering exceeds the force of gravity. Such flares are of special interest in that simulation of their spectra and intensity permits estimating the neutron star parameters.

The spectra of certain soft X-ray transients during quiescence periods exhibit the thermal radiation component of the neutron star located in the system. This allows comparing the cooling curves with observations, as in the case of isolated neutron stars, with the sole difference that the energy release due to accretion must be taken into account. On the one hand, this introduces an uncertainty in the model, but on the other hand it permits verifying theoretical considerations concerning accretion onto the neutron star and thermonuclear transformations of matter in its envelopes.

Of special interest are quasipermanent transients, i.e., those whose active and quiescence periods last a few years or longer. According to the model proposed in [112], the thermal radiation in the quiescence periods is due to the crust cooling after deep heating by accretion. Such cooling is independent of the details of the star structure and composition and therefore its analysis directly yields information on the physics of envelopes. Three sources of this kind are known: KS 1731-260, MXB 1659-29, and AX J175444.2-2754 [113]. The crust of a neutron star is heated during a long period of activity and relaxes to the quasiequilibrium state in the quiescence period that follows, meaning that evolution of the thermal spectrum contains information about the properties of the crust. Therefore, analysis of the thermal luminosity of such an object and its time dependence provides information about heat capacity and thermal conductivity of the crust in the period of activity preceding relaxation and about the equilibrium luminosity at rest. Such data may in turn be used to obtain characteristics of the star as a whole [114].

Estimation of neutron star masses from the Kepler parameters of X-ray binary systems is not yet a reliable method because of theoretical uncertainties, such as those related to the transfer of angular momentum via accretion. The most accurate estimates are obtained for binary systems of two neutron stars due not only to the absence of accretion but also to marked GR effects, whose measurement allows determining the complete set of orbital parameters. Sufficiently accurate mass estimates (with an error $< 0.2M_\odot$) are also available for several binary systems containing a white dwarf as the companion and for the system mentioned in Section 2.1, in which the companion is a main-sequence star. These estimates lie in the range $1.1M_\odot < M < 2M_\odot$.

4. The core of a neutral star and supernuclear density matter

In this section, we focus on the equation of state of the neutron star core, disregarding details of the microscopic theory and nonstationary processes. We note that the Fermi energy of all particles essential for this equation is many orders of magnitude higher than the kinetic thermal energy.

Therefore, a good approximation is given by the equation of state of cold nuclear matter in which the dependence of the pressure on density and temperature, $P(\rho, T)$, is substituted by a one-parametric dependence $P(\rho)$ at $T \to 0$.

4.1 The outer core

Nucleons in the outer core of a neutron star form a strongly interacting Fermi liquid, whereas leptons make up an almost ideal Fermi gas. Therefore, the energy density $\mathcal{E}$ can be represented as the sum of three terms,

$$\mathcal{E}(n_\mathrm{n}, n_\mathrm{p}, n_\mathrm{e}, n_\mu) = \mathcal{E}_\mathrm{N}(n_\mathrm{n}, n_\mathrm{p}) + \mathcal{E}_\mathrm{e}(n_\mathrm{e}) + \mathcal{E}_\mu(n_\mu)\,, \qquad (6)$$

where n_e, n_μ, n_n, and n_p are concentrations of electrons, μ^--mesons, neutrons, and protons. The equations of state and concentration of particles are determined by the energy density minimum at a fixed baryon volume density $n_\mathrm{b} = n_\mathrm{n} + n_\mathrm{p}$ and the electroneutrality condition $n_\mathrm{e} + n_\mu = n_\mathrm{p}$. This implies that the relations $\mu_\mathrm{n} = \mu_\mathrm{p} + \mu_\mathrm{e}$ and $\mu_\mu = \mu_\mathrm{e}$ are satisfied for the chemical potentials μ_j of particles $j = \mathrm{n}, \mathrm{p}, \mathrm{e}, \mu^-$, expressing the equilibrium conditions with respect to the electron and muon beta-decay and beta-capture reactions: $\mathrm{n} \to \mathrm{p} + \mathrm{e} + \overline{\nu}_\mathrm{e}$, $\mathrm{p} + \mathrm{e} \to \mathrm{n} + \nu_\mathrm{e}$, $\mathrm{n} \to \mathrm{p} + \mu + \overline{\nu}_\mu$, and $\mathrm{p} + \mu \to \mathrm{n} + \nu_\mu$, where $\nu_{\mathrm{e},\mu}$ and $\overline{\nu}_{\mathrm{e},\mu}$ are electron and muon neutrinos and antineutrinos. Neutron star matter (unlike the matter of a proto-neutron star, i.e., the collapsed progenitor core, within the first minutes after the supernova explosion) is transparent to neutrinos: therefore, the chemical potentials of neutrino and antineutrino are equal to zero. Electrons at the densities being considered are ultrarelativistic, and therefore $\mu_\mathrm{e} \approx c p_\mathrm{Fe} \approx 122.1\,(n_\mathrm{e}/0.05 n_0)^{1/3}$ MeV, where p_Fe is the electron Fermi momentum and $n_0 = 0.16$ fm^{-3} is the normal nuclear volume density corresponding to the normal mass density ρ_0. In the general case, muons are moderately relativistic, which dictates the use of the general expression $\mu_\mu = m_\mu c^2 \left[1 + (p_\mathrm{F\mu})^2/(m_\mu c)^2\right]^{1/2}$. As soon as the equilibrium is known, the pressure can be found from the equation $P = n_\mathrm{b}^2 \mathrm{d}(\mathcal{E}/n_\mathrm{b})/\mathrm{d}n_\mathrm{b}$.

Thus, the construction of the equation of state for the outer core of a neutron star reduces to the search for the function $\mathcal{E}_\mathrm{N}(n_\mathrm{n}, n_\mathrm{p})$. A number of ways to address this problem have been proposed based on a variety of theoretical physics methods, such as the Brueckner–Bethe–Goldstone theory, the Green's function method, variational methods, the relativistic mean field theory, and the density functional method [25, § 5.9]. The Akmal-Pandharipande–Ravenhall (APR) model known in several variants is currently regarded as the most reliable one [115]. The APR model uses the variational principle of quantum mechanics, under which an energy minimum for the trial wave function is sought. This function is constructed by applying a linear combination of the operators describing admissible symmetry transformations in the coordinate, spin, and isospin spaces to the Slater determinant consisting of wave functions for free nucleons. APR variants differ in the effective nucleon–nucleon interaction potentials used to calculate the mean energy. The potentials borrowed by the authors from earlier publications take the modern nuclear theory into account and their parameters are optimized so as to most accurately reproduce the results of nuclear physics experiments. We note that the addition of an effective three-particle nucleon–nucleon potential to the two-particle one ensures a remarkably close agreement between theory and experiment.

The effective functional of the nuclear matter energy density was used to construct another known equation of state, SLy [116]. Calculations based on the SLy equation are less detailed but easier to use than in the APR model. This equation is constructed in accordance with the same scheme as the well-known FPS equation of state [117], which seems to have been especially popular in the 1990s in calculations of the astrophysical properties of neutron stars. The main difference between SLy and FPS lies in the specification of parameters of the effective energy density functional accounting for current experimental data. An important advantage of both models over many others is their applicability not only to the stellar core but also to the crust, which allows determining the position of the crust–core interface on the density scale in a self-consistent manner [118].

We also note the convenient parameterization for the APR equation of state [119] and explicit fitting expressions for SLy [120] for the dependence of pressure on density and the so-called pseudoenthalpy, a convenient parameter for calculating the properties of rapidly rotating neutron stars [121].

Figure 2 shows $P(\rho)$ dependences for the FPS, SLy, and APR models. Comparison of FPS and SLy shows that a more exact account of current experimental data makes the $P(\rho)$ dependence steeper and the equation of state stiffer. Bold dots correspond to the density in the center of a neutron star with $M = M_\mathrm{max}$ for each of these equations; the segments of the curves to the right of these dots cannot be realized in a static star.

A common drawback of the above models is the use of a Lorentz noninvariant theory in the description of hadrons. Such a description becomes a priori incorrect in the central part of the core, where the speeds of nucleons on the Fermi surface may constitute an appreciable fraction of the speed of light. The same drawback is inherent in all other aforementioned approaches, with the exception of the relativistic mean field theory. This theory, suggested in the 1950s, was especially popular in the 1970s [122]. It has a number of appealing features. Specifically, its Lorentz invariance guarantees the fulfillment of the condition that the speed of sound

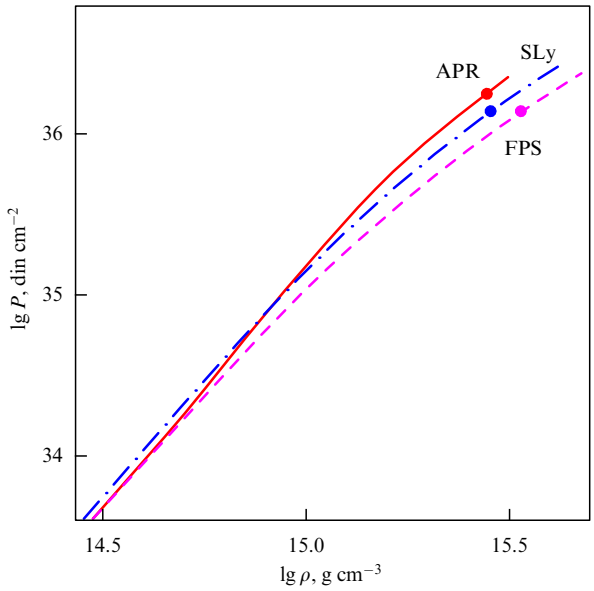

Figure 2. FPS, Sly, and APR equations of state for the core of a neutron star. Bold dots on the curves correspond to the maximally possible density in a stationary star.

does not exceed the speed of light, which is subject to violation in some other models. But the assumption of the spatial uniformity of meson field sources underlying this theory is valid only if $n_b \gg 100\,n_0$ [25]. The matter density necessary for this condition to be satisfied is much higher than that in the interior of a neutron star. Therefore, the equations of state in the core of neutron stars are calculated realistically based on nuclear interaction models that are not Lorentz invariant but are still applicable to the largest part of the stellar core.

Mutual concentrations of different particles need to be known in addition to the $P(\rho)$ dependence. Specifically, the dependence of the proton fraction x_p in the neutron–proton–electron–muon (npeμ) matter on the density ρ is crucial. The fact is that the principal mechanism behind neutrino energy losses in the outer core of a neutron star is the so-called modified Urca processes[2] (abbreviated as Murca by K P Levenfish) consisting of consecutive reactions $n + N \to p + N + e + \bar{\nu}_e$ and $p + N + e \to n + N + \nu_e$, where N = n or N = p is the mediator nucleon (called 'the active spectator' by Chiu and Salpeter [72]). The involvement of the mediator distinguishes the Murca processes from ordinary processes of beta-decay and beta-capture, referred to as direct Urca processes. If $x_p \lesssim x_c$, where the value of x_c varies between 0.111 and 0.148 depending on the muon concentration, the energy and momentum conservation laws cannot be fulfilled simultaneously without the participation of a mediator nucleon in the Urca process, keeping in mind that the momenta of the involved strongly degenerate neutrons n, protons p, and electrons e lie close to their Fermi surfaces [125]. For $x_p > x_c$, direct Urca processes much more powerful than Murca come into play. For this reason, the neutron star suffers enhanced cooling if x_p exceeds x_c in one of its parts.

In different variants of the APR model, x_p grows nonmonotonically from $\approx 0.01-0.02$ at $n_b = n_0$ to $x_p \approx 0.16-0.18$ at $n_b > 1.2$ fm^{-3}. Therefore, if the APR model holds, the density of matter in the center of a massive ($M \gtrsim 1.8 M_\odot$) neutron star is such that it switches on direct Urca processes and speeds up its cooling. In contrast, direct Urca processes are impossible (for stable stars) in the SLy model.

4.2 The inner core and hyperons

Strong gravitational compression in the interior of a neutron star is likely to provoke the conversion of nucleons into hyperons if such conversion may reduce the energy density at a given n_b. The process is mediated by the weak interaction with a change of strangeness (quark flavor). According to modern theoretical models, the conversion is possible at $\rho \gtrsim 2\rho_0$.

The equation of state containing hyperons is calculated as described for the npeμ matter in Section 4.1, but the equations for the chemical potentials are supplemented with new ones for the equilibrium conditions with respect to the weak interactions. The lightest baryons make an octet of two nucleons (p and n with zero strangeness $S = 0$), four hyperons with $S = -1$ (Λ^0, Σ^-, Σ^0, and Σ^+), and two hyperons with $S = -2$ (Ξ^0 and Ξ^-); here, they are listed in the order of increasing mass. Under normal conditions, hyperons decay for fractions of nanoseconds. But in matter composed of degenerate neutrons, μ_n increases as the density increases. When μ_n reaches the minimal chemical potential of a hyperon given by its mass, this hyperon becomes stable because the decay reaction ceases to be thermodynamically favorable.

This requires clarification. Although Λ^0 is the lightest of all hyperons, Σ^- is the first to be stabilized as the density increases because the decay of the Σ^--hyperon yields an electron, in conformity with the equilibrium condition $\mu_{\Sigma^-} = \mu_n + \mu_e$. The electrons, like neutrons, are strongly degenerate, and their chemical potential μ_e is equal to the Fermi energy; the addition of this energy to μ_n permits the equilibrium condition to be satisfied at a smaller density (as was first noticed by Salpeter in 1960 [126]). Similarly, the necessity of subtracting μ_e from μ_n may make the formation of Σ^+ hyperons disadvantageous. However, electrons are gradually replaced by Σ^- hyperons and μ_e decreases as the density increases. Due to this, many theoretical models predict the appearance of Σ^+ hyperons at a sufficiently high density, $n_b \gtrsim 5\,n_0$. In the general case, both electrons and muons are gradually substituted by negatively charged hyperons as the density increases. In the models predicting a high hyperon concentration, leptons disappear at $n_b \gtrsim 1$ fm^{-3} and the so-called 'baryonic soup' is created with high average strangeness per baryon (almost -1 in the central parts of maximum-mass stars).

The current theory lacks a rigorous description of nucleon–hyperon and hyperon-hyperon interactions. This uncertainty is aggravated by the uncertainty arising from the choice of the mode of description of multiparticle interactions; this results in a great variety of model equations of state for the inner core of a neutron star. Figure 3 exemplifies three

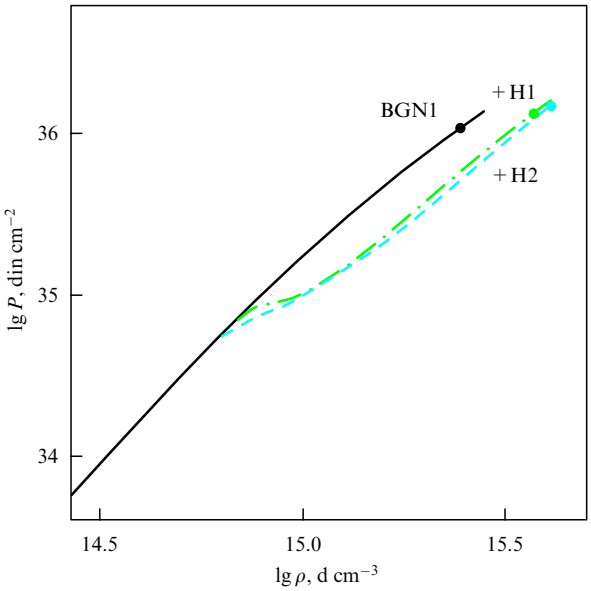

Figure 3. Equations of state for the core of a neutron star according to the variants of the model proposed in [127] with (BGN1H1 and BGN1H2) and without (BGNI) hyperons. Bold dots on the curves indicate the maximally possible density in a stationary star. The data and notations are borrowed from [25].

[2] The term Urca process was coined by G A Gamov and M Schönberg. Gamov recalled [124]: "We called it the Urca process partially to commemorate the casino in which we first met and partially because the Urca process results in a rapid disappearance of thermal energy from the interior of a star similar to the rapid disappearance of money from the pockets of the gamblers in the Casino da Urca. Sending our article on the Urca process for publication in the Physical Review, I was worried that the editors would ask why we called the process 'Urca'. After much thought I decided to say that this is the short for unrecordable cooling agent, but they never asked."

of the equations of state proposed in [127]. The solid curve corresponds to the so-called minimal model disregarding hyperons. The dashed and dashed-dotted curves correspond to two models with hyperons. If the density exceeds the threshold for the appearance of new particles, the equation of state is noticeably softened, as is natural when part of the strongly degenerate high-energy neutrons are replaced by slow heavy hyperons. However, the magnitude of the effect depends on the details of hyperon–nucleon and hyperon–hyperon interactions.

4.3 Phase transformations and deconfinement

As the density ρ increases above the nuclear density ρ_0, matter may undergo phase transitions to qualitatively new states, regarded as exotic from the standpoint of terrestrial nuclear physics; the very existence of these states depends on the concrete features of strong interactions and the quark structure of baryons.

4.3.1 Meson condensation. It has been known since the mid-1960s [71] that the core of a neutron star must contain π mesons (pions), i.e., the lightest mesons. Bose condensation of pions in nuclear matter is usually hampered by strong pion–nucleon repulsion. However, it was shown in [128–131] that collective excitations (pion-like quasiparticles) may arise in a superdense medium and condense with the loss of translational invariance. Further studies revealed the possibility of creating different phases of the pion condensate and the importance of correlations between nucleons for its existence. It was shown that short-range correlations and the formation of ordered structures in dense matter interfere with pion condensation [132].

Kaons (K mesons) are the lightest strange mesons. They appear in the core of a neutron star as a result of the processes $e + N \to K^- + N + \nu_e$ and $n + N \to p + K^- + N$, where N is a nucleon whose participation ensures the momentum and energy conservation in the degenerate matter. The possibility of Bose condensation of kaons at $\rho \gtrsim 3\rho_0$, first understood in the 1980s [133], has thereafter been studied by many authors (see [134]). In a neutron star, it involves K^--like particles, by analogy with pion condensation. These particles have a smaller mass than isolated K mesons; it is this property that makes their Bose condensation possible. A method for the theoretical description of the kaon condensate taking the effects of strong interaction in baryonic matter into account was developed in [135]. Formation of the kaon condensate depends on the presence of hyperons and strongly affects the properties of the nucleon component of matter. Kaon condensation, like pion condensation, is accompanied by the loss of translational invariance. The condensate forms via first- and second-order phase transitions, depending on the strength of the force of attraction between kaons and nucleons [136]. Both pion and kaon condensations make the equation of state much softer.

4.3.2 Quark deconfinement. Because hadrons are made of quarks, the fundamental description of dense matter must take the quark degrees of freedom into account. Quarks cannot be observed in a free state when their density is low because they are held together (confinement) by the binding forces enhanced at low energies [137]. As the density (and hence the characteristic energies of the particles) grows, baryons fuse to form quark matter. In 1965, Ivanenko and Kurdgelaidze [138] suggested that neutron stars must have quark cores. With the advent of quantum chromodynamics, calculations of quark matter properties were performed in terms of the perturbation theory using the noninteracting quark model as the initial approximation [139, 140]. However, the use of this theory is limited to energies $\gg 1$ GeV, while the chemical potential of particles in neutron stars does not reach such high values. More quark matter models were proposed, and the superfluidity of this matter associated with quark Cooper pairing was considered (see the references in [25, § 7.5]). These models were used to explore quark stars and hybrid stars, i.e., neutron stars with cores made of quark matter [2]. The authors of [141] predicted a series of phase transitions in the interior of a hybrid star with sequential deconfinement of quark flavors at $n_b \sim 0.25$, $0.5-0.8$, and $1.1-1.8$ fm^{-3}.

All published models of phase transitions in the cores of neutron stars have serious drawbacks. The quark and baryonic phases are typically treated in the framework of different models and cannot therefore be described self-consistently. Calculations from the perturbation theory are unrealistic at those relatively small densities at which they predict a phase transition. For this reason, the existence of a quark core in neutron stars cannot be proved theoretically. However, it may be hoped that this goal will be achieved based on the analysis of observations of compact stars.

4.3.3 Mixed phases. First-order phase transitions can be realized via a state in which one phase co-exists with another in the form of droplets. Such phase transitions, called non-congruent [142], have been considered in connection with compact stars since the 1990s [143]. The coexistence of two phases in the core of a neutron star is possible thanks to the abandonment of the implicit assumption of electroneutrality of each individual phase. In the mixed phase, the electric charge of one component is on the average compensated by that of the other, and the matter structure is determined by the balance of surface tension at the boundaries between droplets, the energy density of baryonic matter, the kinetic energy of the constituent particles, and electrostatic energy. Mixed states are feasible for both meson condensation and baryon dissociation into quarks.

4.3.4 Crystalline core. The early models of neutron stars assumed that strong short-range neutron–neutron repulsion results in the formation of the solid inner core of a neutron star [144] as suggested in review [19] by Ginzburg. In subsequent works, it was taken into account that the nucleon–nucleon interaction occurs by an exchange of vector mesons, which gives rise to the effective Yukawa potential. As the calculations became more exact by the late 1970s, it was understood that the realistic effective potentials of neutron–neutron interactions do not lead to crystallization [145].

An alternative possibility of crystallization arises from the tensor component of the mid-range nucleon–nucleon attraction [146]. It was shown in [147] that tensor interaction can lead to structures in which neutrons are located in a plane with oppositely oriented spins, each such plane hosting oppositely directed proton and neutron spins (so-called alternating spin (ALS) structures). If the gain in the binding energy during formation of an ALS structure exceeds the loss of the kinetic energy of the particles, then the structure may become energetically favorable and a phase transition into this state occurs.

Moreover, given a low enough abundance of protons in baryonic matter, $x_p \lesssim 0.05$, their localization may occur, accompanied by modulation of the neutron density [148]. Under certain conditions, mixed phases may also be just ordered into periodic structures (see monograph [2] and the references therein).

In other words, there are numerous hypotheses regarding the structure and composition of the neutron star core, differing in details of microscopic interactions and theoretical models for their description. We consider how they treat the parameters of neutron stars.

4.4 Relation to observations

Manifestations of the properties of a neutron star core can be arbitrarily categorized into dynamic and quasistatic. The former are due to relatively fast processes inside the star. For example, a phase transition in the inner core may occur not only at the star birth but also as it goes through its evolution, e.g., during cooling (when the temperature decreases to below the critical one) or rotation slowdown (when the central pressure increases due to a reduction in centrifugal forces). Such a phase transition leads to a starquake with the release of thermal energy, a burst of neutrinos, excitation of crustal oscillations, and an abrupt change in the rotational velocity due to the altered moment of inertia [54]. All these effects could be possible to record and measure under favorable conditions. The authors of [149] attributed sharp jumps of pulsar rotational periods (glitches) to such phase transitions. Starquakes and glitches may be a consequence of occasional adjustment of the crust rotational velocity to the rotation rate of the superfluid component of the nucleon liquid [19, 52, 55].

Quasistatic manifestations include, inter alia, the effects of the core structure and the physical properties of its superdense matter on the theoretical radius and cooling rate of the star. The influence on the cooling, and hence the effective surface temperature, originates from the difference in the rates and mechanisms of neutrino losses in individual core models [26, 30]. The influence on the relation between the stellar radius R and the mass M is realized via the function $P(\rho)$ in accordance with the TOV equation. Figure 4 exemplifies the $R(M)$ dependence for six equations of state of the neutron stars shown in Figs 2 and 3 and one equation for a quark (strange) star (with the use of data from [25]). It can be seen that quark stars are expected to have smaller masses and radii than typical neutron stars. Solid dots at the ends of the curves correspond to the maximum mass of a stationary star for each equation of state. If a neutron star of a higher mass is discovered, the equation in question can be discarded.

There are general theoretical constraints on the possible values of masses and radii, besides the equations of state. Evidently, the radius R of any star must not be smaller than r_g; otherwise, we are dealing with a black hole. Moreover, it can be shown [25] that the condition $v_s < c$, where v_s is the speed of sound in a local reference frame and c is the speed of light in the vacuum, imposed by the special theory of relativity and the causality principle requires that the relation $R > 1.412\, r_g$ be satisfied, which excludes the point (M, R) from entering inside the hatched triangle in Fig. 4.

An additional limitation is needed for the gravitation of a rotating star to overcome the centrifugal acceleration. Clearly, the radius must not be too large. In Fig. 4, the largest values of the radius in the dependence on the mass M at a given rotation period P are shown by alternating short and long dashes for $P = 1$ ms, 1.4 ms, and 0.5 ms. It can be seen that the period $P = 1.2$ ms (the shortest period observed to date) does not place any serious constrains on R. On the other hand, the pulsar period 0.5 ms is incompatible with any of the known theoretical equations of state of dense matter (the detection of such a period in the radiation from the 1987A supernova remnant was reported in 1989 [150], but it later proved to be a technical error [151]).

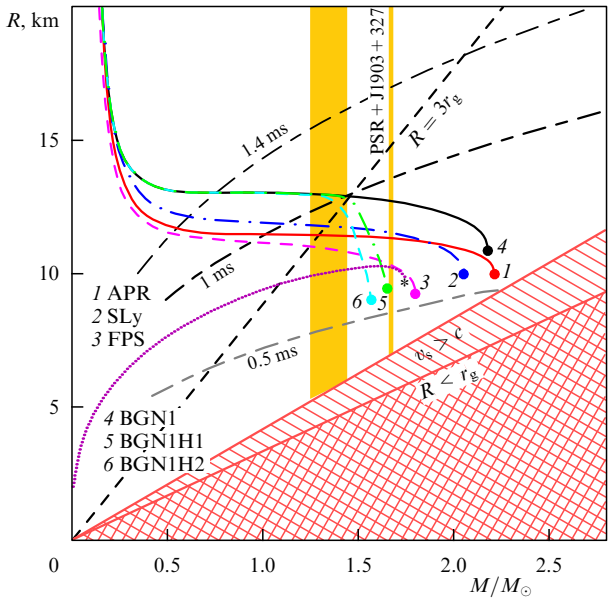

Figure 4. Mass dependence of the compact star radius. Curves *1–6* correspond to the equations of state of neutron stars shown in Figs 2 and 3. The dotted curve corresponds to one of the feasible equations of state of a quark star. The hatched triangular area is forbidden by the causality principle. The crosshatched triangular area lies below the event horizon. Three short- and long-dashed curves show additional constraints for rotating neutron stars: the area under the corresponding curve is permitted at the rotation periods indicated (1.4, 1, and 0.5 ms). The straight line $R = 3r_g$ corresponds to the minimal stability radius of the circular orbit of a test particle around the neutron star of a given mass. The wide vertical strip encompasses the masses of binary neutron stars measured with an error less than $0.1M_\odot$ at the 2σ level [25]; the narrow vertical strip corresponds to the mass of the PSR J1903 + 0327 millisecond pulsar [42] (see the Note added in proof).

The wide vertical strip in Fig. 4 depicts the range of exactly measured masses of neutron stars in binary systems made up of a pulsar and a neutron star The narrow vertical strip corresponds to the estimated mass of PSR J1903 + 327 mentioned in Section 2.1. Confirmation of this estimate would make the choice between theoretical models much more definitive. For example, it follows from the figure that the existence of a star of such mass implies the absence of hyperons in the model [127].

If R and M were known exactly for a certain compact star, it would probably permit choosing one of the equations of state as the most realistic one. Unfortunately, the current accuracy of measurement of neutron star radii leaves much to be desired. Determination of stellar masses and radii requires a reliable theoretical description of the envelopes that influence the star surface temperature and the formation of the emitted radiation spectrum. We return to this issue in Section 7.5.

5. Envelopes

Envelopes of a neutron star are divisible into the solid crust in which atomic nuclei are arranged into a crystal and the liquid ocean composed of the Coulomb fluid. The crust is subdivided into the inner and outer parts. In the former, the nuclei are embedded in a sea of free neutrons and electrons, while the latter contains no free neutrons. A neutron star may have a gaseous plasma atmosphere at the shell–vacuum interface, while its core is surrounded by a liquid crystal mantle topped by the crust.

5.1 Inner crust

The inner crust is normally $\sim 1-2$ km thick. Its density increases from $\rho_{\rm drip} \approx (4-6) \times 10^{11}$ g cm^{-3}, at which neutrons begin to 'drip' out of nuclei, to $\sim 0.5\rho_0$, when the atomic nuclei fuse into a homogeneous mass. The nuclear chemical equilibrium with respect to beta-capture and beta-decay reactions in the inner crust accounts for the matter composition that cannot be reproduced under laboratory conditions (neutron-rich heavy nuclei embedded in a fluid composed of neutrons and electrons). The physics of such matter is fairly well described in [152]. The neutrons in a large portion of the inner crust are superfluid; according to theoretical estimates, the critical superfluidity temperature varies with density and reaches billions of degrees or an order of magnitude higher than the typical kinetic temperature of matter in the inner crust of a neutron star.

The pressure in the inner crust of a neutron star is largely created by degenerate neutrons. However, superfluidity may decrease their heat capacity and is therefore responsible for the decisive contribution of atomic nuclei to the thermal capacity of the inner crust. The nuclei make up a crystal lattice, formed essentially by Coulomb interaction forces (a Coulomb or Wigner crystal). An adequate description of their contribution is possible by considering collective vibrational excitations (phonon gas). Because the electrons are relativistic and highly degenerate particles, their contribution to the heat capacity of the inner crust is insignificant unless the temperature is very low. However, it may appreciably increase when the temperature of the Coulomb crystal decreases much below the Debye temperature, imposing a 'freeze-out' on phonon excitations [25, § 2.4.6].

The electric conductivity in the inner crust is largely due to electrons, whose scattering plays an important role. The scattering on phonons of a crystal lattice prevails at relatively high temperatures, and that on lattice defects or admixtures is responsible for the residual resistance at low temperatures. Ions (atomic nuclei) incorporated into the crystal lattice make no appreciable contribution to conductance. At the same time, thermal conductivity is due to phonons and neutrons, besides electrons whose scattering is governed by the same mechanisms that operate in the case of electric conductivity supplemented by electron–electron collisions. Phonons may become the main heat transfer agents in the presence of lattice defects and admixtures hampering the participation of electrons in this process [153]. Neutrons, especially superfluid ones, may also serve as heat carriers in the inner crust [154].

5.2 Mantle

The core of a neutron star may be separated from the bottom of its inner crust by a layer that contains exotic atomic nuclei and is called the mantle [155]. In the low-density liquid droplet model, the spherical shape of the atomic nucleus is energetically advantageous; it minimizes the surface energy, but the contribution from the Coulomb energy at a higher density may change the situation. The mantle consists of a few layers containing such phases of matter in which atomic nuclei are shaped not like spheres but rather likes cylinders (the so-called 'spaghetti' phase), plane-parallel plates ('lasagna' phase), or 'inverse' phases composed of nuclear matter with entrapped neutron cylinders ('tubular' phase) and balls ('Swiss cheese' phase) [152]. Such structures for collapsing cores of supernovae were first conjectured in [156] and for neutron stars in [157]. The mantle has properties of a liquid crystal [155], whereas spherical nuclei give rise to a three-dimensional crystal lattice. Direct Urca processes of neutrino emission are allowed in the mantle, although they are unfeasible in other star envelopes; their high intensity [158] may promote cooling of the neutron star.

Not all current equations of state of nuclear matter predict the mantle; some of them treat such a state as energetically unfavorable. The mantle appears in the FPS model, but not in the most modern SLy model.

5.3 Outer crust and its melting

The outer shells of a neutron star are hundreds of meters thick and consist of an electron–ion plasma that is completely ionized (i.e., consists of ions in the form of atomic nuclei and strongly degenerate free electrons), probably except a several-meter-thick outer layer with the density below 10^6 g cm^{-3}. The total pressure is determined by the pressure of degenerate electrons. The electrons become relativistic (with the Fermi momentum $p_{\rm F}$ comparable to $m_{\rm e}c$, where $m_{\rm e}$ is the electron mass) at $\rho \gg 10^6$ g cm^{-3} and ultrarelativistic ($p_{\rm F} \gtrsim m_{\rm e}c$) at $\rho \gg 10^6$ g cm^{-3}. At such densities, ions give rise either to a Coulomb liquid (whose properties mostly depend on Coulomb interactions between ions) or to a Coulomb crystal.

The electron Fermi energy in deep-lying layers of the outer envelopes increases so as to enrich nuclei with neutrons by virtue of beta-captures. Finally, the inner–outer crust interface forms at $\rho = \rho_{\rm drip}$, where free neutrons appear.

The external boundary of the outer crust normally coincides with the crystallization point of the Coulomb liquid making up the neutron star ocean. The position of this point is given by the density dependence of the Coulomb crystal melting temperature. In the so-called one-component Coulomb plasma model disregarding electron–ion interactions and treating ions as classical point particles, formation of the Coulomb crystal is defined by the equality $\Gamma = 175$ or (in a more realistic approach) $\Gamma \sim 100-200$ [159]. Here, $\Gamma = (Ze)^2/(ak_{\rm B}T)$ is the Coulomb coupling parameter characterizing the relation between the potential Coulomb energy of the ion and their kinetic energy, $a = (4\pi n_{\rm i}/3)^{-1/3}$ is the radius of the ion sphere, $n_{\rm i}$ is the ion volume density, and $k_{\rm B}$ is the Boltzmann constant. The melting point for a typical neutron star envelope lies at $\rho_{\rm m} \sim 10^6-10^9$ g cm^{-3}, depending on its thermal structure (i.e., temperature variations with depth related to the star age and past history). However, a cold enough neutron star may lose both the atmosphere and the ocean in a superstrong magnetic field; in such a case, the external boundary of the crust coincides with the stellar surface (see [160] and the references therein).

5.4 Ocean

The bottom of the neutron star ocean is located at the melting point with the density $\rho_{\rm m}$, while its surface is arbitrary because

of the lack of a clear-cut ocean–atmosphere interface on a typical star. An exception, as in the case of the solid crust, is neutron stars having a rather strong magnetic field, which may be responsible for the absence of an optically thick atmosphere and its substitution by a liquid boundary. Most of the ocean consists of atomic nuclei surrounded by degenerate electrons. Therefore, in the general case, we speak of ions surrounded by electrons, with the understanding that ions mean both completely and partially ionized atoms.

The ocean matter is a Coulomb liquid, most of which is strongly coupled, i.e., $\Gamma \gg 1$. One of the main problems in theoretical studies of such matter is adequate consideration of the influence of microscopic correlations between ion positions on the macroscopic physical characteristics of the matter being investigated, such as equations of state [159] and kinetic coefficients [161].

5.5 Atmosphere

The stellar atmosphere is a layer of plasma in which the thermal electromagnetic radiation spectrum is formed. The spectrum contains valuable information about the effective surface temperature, gravitational acceleration, chemical composition, magnetic field strength and geometry, and mass and radius of the star. The geometric thickness of the atmosphere varies from a few millimeters in relatively cold neutron stars (effective surface temperature $T_{\rm eff} \sim 10^{5.5}$ K) to tens of centimeters in rather hot ones ($T_{\rm eff} \sim 10^{6.5}$ K). In most cases, the density of the atmosphere gradually (without a jump) increases with depth; however, as mentioned above, stars with a very low effective temperature or superstrong magnetic field have either a solid or a liquid condensed surface.

The deepest layers of the atmosphere (its 'bottom' defined as a layer with the optical thickness close to unity for the majority of outgoing rays) may have the density ρ from $\sim 10^{-4}$ to $\sim 10^{6}$ g cm^{-3} depending on the magnetic field B, the temperature T, the acceleration of gravity g, and the chemical composition of the surface. The presence in the atmosphere of atoms, molecules, and ions having bound states substantially alters absorption coefficients of electromagnetic radiation and thereby the observed spectrum.

Although the neutron star atmosphere has been investigated by many researchers for several decades, these studies (especially concerning strong magnetic fields and incomplete ionization) are far from being completed. For magnetic fields $B \sim 10^{12} - 10^{14}$ G, this problem is practically solved only for hydrogen atmospheres with $T_{\rm eff} \gtrsim 10^{5.5}$ K [162, 163]. The bound on $T_{\rm eff}$ from below is related to the requirement of smallness of the contribution from molecules compared to that from atoms, the quantum mechanical properties of molecules in a strong magnetic field being poorly known. For $B \sim 10^{12} - 10^{13}$ G and $10^{5.5}$ K $\lesssim T_{\rm eff} \lesssim 10^{6}$ K, there are models of partly ionized atmospheres composed of carbon, oxygen, and nitrogen [164] in which a bound on $T_{\rm eff}$ from above arises from the rough treatment of ion motion effects across the magnetic field that holds at low thermal velocities (see Section 6.3).

6. Magnetic fields

6.1. Magnetic field strength and evolution

As discussed in the Introduction, the majority of currently known neutron stars have magnetic fields unattainable in terrestrial laboratories, with typical values $B \sim 10^{8} - 10^{15}$ G at the surface, depending on the star type. The field strength inside a star can be even higher. For example, certain researchers propose explaining the energetics of AXP and SGR in terms of core magnetic fields as high as $B \sim 10^{16} - 10^{17}$ G at the birth of the neutron star (see [165] and the references therein). The theoretical upper bound obtained numerically in [121] is consistent with the estimate from the virial theorem [166, 167]: $\max(B) \sim 10^{18}$ G.

A number of theoretical models of field generation have been proposed suggesting the participation of differential rotation, convection, magneto-rotational instability, and thermomagnetic effects either associated with supernova explosion and collapse or occurring in young neutron stars (see [168]). Specifically, the "$\alpha - \Omega$-dynamo model" [169, 170] assumes that the core of a neutron star born with a sufficiently short (millisecond) rotation period acquires a toroidal magnetic field up to $B \sim 10^{16}$ G due to differential rotation, while the pulsar magnetic field is generated by means of convection at the initial rotation periods $\gtrsim 30$ ms. However, none of the proposed models is able to account for the totality of currently available neutron star data.

Electric currents maintaining the stellar magnetic field with the involvement of differential rotation circulate either in the inner crust or in the core of a neutron star, i.e., where the electric conductivity is high enough to prevent field decay for a time comparable with the age of known pulsars. It was shown as early as 1969 [171] that the characteristic time of Ohmic decay of the core magnetic field may exceed the age of the Universe. For a magnetic field originating in the core of a neutron star, proton superconductivity gives rise to the field existing in the form of quantized magnetic tubes (Abrikosov vortices, or fluxoids) with a microscopic transverse dimension.

The magnetic field of a neutron star changes in the course of its evolution, depending on many factors and inter-related physical processes (see, e.g., [172] and the references therein). Specifically, the field undergoes Ohmic decay and a change in configuration under the effect of the Hall drift; also, magnetic field lines reconnect during starquakes. Thermoelectric effects, as well as the dependence of components of the thermal and electrical conductivity tensors, and plasma thermoelectric coefficients on temperature and the magnetic field, are responsible for the interrelation between magnetic and thermal evolution [98, 99]. Moreover, accretion may strongly influence the near-surface magnetic field [21, 172].

The evolution of a magnetic field generated by Abrikosov vortices is to a large extent dependent on their interaction with other core components, such as Feynman–Onsager vortices in the neutron superfluid [6, 171], and conditions at the core boundary, i.e., interactions of these vortices with crustal matter [55].

6.2 Landau quantization

The motion of free electrons transversally to the field is quantized into Landau levels [173]. Their characteristic transverse scale is the magnetic length $a_{\rm m} = (\hbar c/eB)^{1/2}$ and the interlevel distance in a nonrelativistic theory is the cyclotron energy $\hbar\omega_{\rm c} = 11.577\, B_{12}$ keV, where $\omega_{\rm c} = eB/m_{\rm e}c$ is the electron cyclotron frequency (the notation $B_{12} = B/10^{12}$ G is introduced here). The dimensionless parameters characterizing a magnetic field in relativistic

units b and atomic units γ are

$$b = \frac{\hbar\omega_c}{m_e c^2} = \frac{B_{12}}{44.14}\,, \tag{7}$$

$$\gamma = \left(\frac{a_B}{a_m}\right)^2 = \frac{\hbar\omega_c}{2\,\mathrm{Ry}} = \frac{\hbar^3 B}{m_e^2 c e^3} = 425.44 B_{12}\,, \tag{8}$$

where a_B is the Bohr radius. We call a magnetic field strong if $\gamma \gg 1$ and superstrong if $b \gtrsim 1$. In the relativistic theory, the energies of Landau levels are $E_N = m_e c^2 (\sqrt{1 + 2bN} - 1)$, where $N = 0, 1, 2, \ldots$.

In a superstrong field, specific effects of quantum electrodynamics, such as the electron–positron vacuum polarization in an electromagnetic wave field, become significant. As a result, the vacuum acquires the properties of a birefringent medium, which, at $b \gtrsim 1$, markedly affects the radiation spectrum formed in the atmosphere of a neutron star [174, 175].

For ions with the charge Ze and mass $m_i = Am_u$, where $m_u = 1.66 \times 10^{-24}$ g is the atomic unit of mass, the cyclotron frequency is $\omega_{ci} = |Ze|B/m_i c$, the cyclotron energy is $\hbar\omega_{ci} = 6.35\,(Z/A)\,B_{12}$ eV, and the parameter characterizing the role of relativistic effects is $b_i = \hbar\omega_{ci}/m_i c^2 = 0.68 \times 10^{-8}\,(Z/A^2)\,B_{12}$. The smallness of b_i permits ignoring the relativistic effects for ions in the atmosphere of a neutron star.

The motion of electrons along a circular orbit in a magnetic field in the classical theory leads to cyclotron radiation at the frequency ω_c and the formation of a cyclotron line in the magnetic atmosphere. In quantum theory, the cyclotron line corresponds to transitions between the adjacent Landau levels. Transitions between distant Landau levels result in the formation of cyclotron harmonics with energies E_N. The discovery of the first cyclotron line with the energy 58 keV in the spectrum of the X-ray pulsar in the binary Hercules X-1 [176] in 1978 gave a stunning argument in favor of the idea of neutron star magnetic fields. A number of similar systems with synchrotron lines are known presently. The spectra of several X-ray pulsars in binary systems exhibit cyclotron harmonics with $N \geqslant 1$ [177, 178]; the observation of up to four harmonics has been reported [179].

The spectra of isolated neutron stars may likewise contain cyclotron lines. Electron cyclotron lines can be seen in the thermal spectral range from 0.1 to 1 keV at $B \sim 10^{10} - 10^{11}$ G and ion cyclotron lines at $B \sim 10^{13} - 10^{14}$ G. It is believed that absorption lines in the spectrum of CCO 1E 1207.4-5209 can be attributed to the cyclotron mechanism [180, 181]. We emphasize that ion cyclotron harmonics, unlike electron ones, are too weak to be observed [96].

The effect of Landau quantization on plasma properties is significant when the cyclotron energy is not too small compared with the thermal ($k_B T$) and Fermi (ϵ_F) energies. If $\hbar\omega_c$ is much higher than these two energies, most electrons in thermodynamic equilibrium are at the ground Landau level. In this case, the field is called strongly quantizing. If $k_B T$ or ϵ_F is much greater than the energy difference between the adjacent Landau levels, the field is a nonquantizing one. The smallness condition on the thermal energy compared with the cyclotron one can be written as $\hbar\omega_c/k_B T \approx 134\,B_{12}/T_6 \gg 1$ for electrons and as $\hbar\omega_{ci}/k_B T \approx 0.0737\,(A/Z)\,B_{12}/T_6 \gg 1$ for ions. The second condition (higher $\hbar\omega_c$ than ϵ_F) imposes a bound on density. Degenerate electrons occur at the ground Landau level if their concentration n_e is lower than

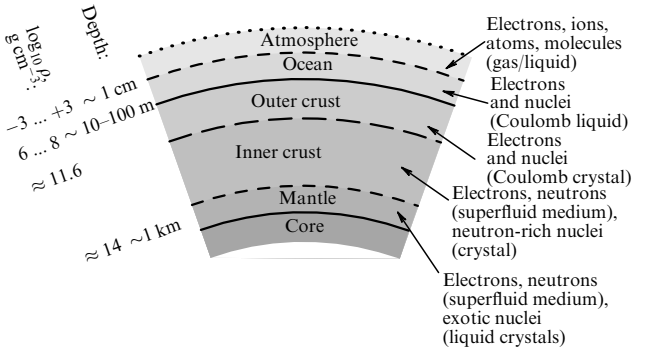

Figure 5. Schematic cross section of neutron star envelopes. From bottom up: core, mantle, inner crust, outer crust, ocean, atmosphere. Right-hand side: composition of these layers; left-hand side: characteristic values of density logarithm and depth from the surface.

$n_B \equiv (\pi^2\sqrt{2}\,a_m^3)^{-1}$. Therefore, the field is strongly quantizing at $\rho < \rho_B$, where

$$\rho_B = \frac{m_i n_B}{Z} \approx 7 \times 10^3 \left(\frac{A}{Z}\right) B_{12}^{3/2}\ \mathrm{g\,sm^{-3}}\,. \tag{9}$$

The field is weakly quantizing at $\rho > \rho_B$ and nonquantizing at $\rho \gg \rho_B$. Estimates analogous to (9) are also easy to obtain for other fermions [25, § 5.17].

We note that a nonquantizing magnetic field has no effect on the equation of state (Bohr–van Leeuwen theorem). It follows from Fig. 5, taking account of relation (9), that magnetic fields inherent in neutron stars are strongly quantizing in the atmosphere and can be quantizing in both the ocean and the outer crust; however, even at limit values $B \sim 10^{18}$ G, the magnetic fields do not affect the stellar core equation of state. These conclusions are based on simple estimates, but they are confirmed by calculations of the nuclear matter equation of state in superstrong magnetic fields [182].

6.3 Atoms and ions in magnetic atmospheres

The atmosphere of a neutron star contains atoms, molecules, and atomic and molecular ions having bound states. Strong magnetic fields markedly affect their quantum mechanical properties (see reviews [160, 183, 184]). It was suggested soon after the discovery of pulsars [185] that at equal temperatures, there should be more atoms in the neutron star atmosphere at $\gamma \gg 1$ than at $\gamma \lesssim 1$ because in a strong magnetic field, the binding energies of their ground state and a certain class of excited states (so-called tightly bound states) markedly increase and the quantum mechanical size decreases. In each of these states, the electron cloud acquires the form of an extended ellipsoid of rotation with the characteristic small semiaxis $a_m = a_B/\sqrt{\gamma}$ and the large semiaxis $l \sim a_B/\ln\gamma \gg a_m$. For example, the binding energy of the ground state of a hydrogen atom at $B \sim 10^{11} - 10^{14}$ G is roughly estimated as $E \sim 200\,(\ln B_{12})^2$ eV (the exact fitting formulas for the energies and other characteristics of hydrogen atoms in a magnetic field are given in [186]).

The properties of molecules and even the very existence of some of their types in strong magnetic fields are poorly known, although they have been discussed for almost 40 years. Those diatomic molecules are fairly well studied whose axis coincides with the direction of the magnetic field. For obvious reasons, the H_2 molecule has been thoroughly

investigated. The approximate formulas for its binding energy at $\gamma \gtrsim 10^3$ increasing at the same rate $\propto (\ln\gamma)^2$ as the binding energy of H atoms are presented in [160]. Interestingly, however, numerical calculations in [187] show that this molecule is unstable in a moderate magnetic field (in the range $0.18 < \gamma < 12.3$). Also, the H_2^+ ion has been studied fairly well (see, e.g., [188]); HeH^{++}, H_3^{++}, and other exotic molecular ions becoming stable in strong magnetic fields were considered in [189].

A strong magnetic field can stabilize polymer molecular chains aligned along magnetic field lines. These chains can then be attracted to one another via dipole–dipole interactions and make up a condensed medium. Such a possibility was first postulated by Ruderman in 1971 [185]. Investigations in the 1980s–2000s showed that in fields $B \sim 10^{12}$–10^{13} G, the chains are formed only of H through C atoms and not other elements, and undergo polymerization into a condensed phase either in a superstrong field or at a relatively low temperature, with the sublimation energy of such a condensate being much smaller than predicted by Ruderman (see [190] and the references therein).

The overwhelming majority of researchers of atoms and molecules in strong magnetic fields have considered them to be at rest. Moreover, in studying electron shells, the atomic nuclei were almost universally assumed to be infinitely massive (fixed in space). Such an approximation is a gross simplification for magnetic atmospheres. Astrophysical simulations must take the finite temperature and therefore thermal motion into account. Atomic motion across magnetic field lines breaks the axial symmetry of a quantum mechanical system. At $\gamma \gg 1$, specific effects associated with the collective motion of a system of charged particles become significant. Specifically, the decentered states can be populated in which electrons are mainly located in a 'magnetic well' far from the Coulomb center. These exotic states were predicted for hydrogen atoms in [191]; the same authors and those of [192] were the first to study their energy spectra.

Even at low temperatures, when the thermal motion of atoms can be neglected in the first approximation, the finite mass of the atomic nucleus should be taken into consideration, even in a sufficiently strong field; the nucleus undergoes oscillations in a magnetic field due to Landau quantization even if the generalized momentum [183] describing the motion of the center of mass across the field is zero. Different quantum numbers of an atom correspond to different vibrational energies that are multiples of the cyclotron energy of the atomic nucleus. In a superstrong field, this energy becomes comparable to the electron shell energies and cannot therefore be disregarded.

A comprehensive calculation of the hydrogen atom energy spectrum with the effects of motion across a strong magnetic field taken into account was carried out in [193, 194], and the calculation of the probability of different types of radiative transitions and absorption coefficients in neutron star atmospheres in a series of studies was reported in [95]. Based on these data, a model of the hydrogen atmosphere of a neutron star with a strong magnetic field [162] was elaborated. A database for astrophysical calculations was created using this model in [163].

The quantum mechanical effects of He^+ ion motion were considered in [195, 196]. This case is essentially different from that of a neutral atom in that the values of the ion generalized momentum are quantized [183]. For many-electron atoms, molecules, and ions, the effects of motion across the magnetic field remain unexplored. The perturbation theory applicable to the case of small generalized momenta [197, 198] may prove sufficient to simulate relatively cold atmospheres of neutron stars [164].

6.4 Electron heat and charge transfer coefficients

The magnetic field affects the kinetic properties of the plasma in a variety of ways (see [199]). Any magnetic field makes the transfer of charged particles (in our case, electrons) anisotropic. It hampers their motion and thereby heat and charge transfer by electrons in the direction perpendicular to the field, thus generating Hall currents. These effects are essential when the cyclotron frequency ω_c is much higher than the effective collision frequency, while the latter remains unaltered in a nonquantizing field.

A quantizing magnetic field exerts a more pronounced influence on the transfer process. In a weakly quantizing field (in the presence of degeneracy), kinetic coefficients oscillate with variations of matter density about the values they would have in the absence of quantization. In a strongly quantizing magnetic field, the values of the kinetic coefficients are substantially different from classical ones.

The effects of quantizing magnetic fields on electron transfer in plasma have been studied by different authors for many decades (see the references in [199]). The formulas for electron kinetic coefficients of a completely ionized plasma convenient to use in astrophysics at arbitrary ρ, B, and T were derived in [200]. They were used to calculate thermal evolution of neutron stars as described in the next section.

Figure 6 exemplifies the dependences of heat conductivity coefficients along and across a magnetic field at the plasma characteristics inherent in the thermoinsulating shell of a neutron star with the field $B = 10^{14}$ G; the accurately computed characteristics (solid curves) are compared with the simplified models used in astrophysics previously. The dashed lines represent models disregarding Landau quantization under the assumption of a strong electron degeneracy (to the right of the vertical dashed-dotted line) or nondegeneracy (to the left of the vertical line). The dotted line is the assumption under which thermal spread of electron energies near the Fermi energy is neglected (see [201] for the details and references).

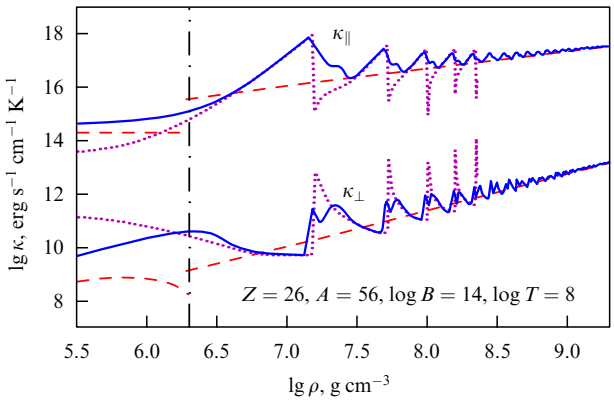

Figure 6. Longitudinal || and transverse ⊥ heat capacities in the iron outer envelope of a neutron star at $T = 10^8$ K and $B = 10^{14}$ Gs [201]. Solid curves are calculations according to [200], dashed lines are the classical model, the dotted line is the results neglecting thermal averaging. Electrons are degenerate to the right of the vertical dashed-dotted line, whose position corresponds to the equality $\epsilon_F = k_B T$.

7. Cooling and thermal radiation

7.1 Cooling stages

About 20 s after its birth, a neutron star becomes transparent to neutrino emission [44], carrying away the energy to outer space and cooling the star. Soon after that, the temperature distribution in the stellar core characterized by high heat conductivity reaches equilibrium, preserved thereafter throughout the star lifetime (probably except for short periods after catastrophic phase transitions in the core postulated by certain hypothetical models). In line with GR, the equilibrium temperature increases toward the center of the star in proportion to $\exp(-\Phi)$, where Φ is the metric function defined by the star hydrostatic model and related to the temporal component of the metric tensor $g_{00} = \exp(2\Phi)$, decreasing from the surface to the center [202].

The stellar crust is for some time hotter than the core. The cooling wave reaches the surface within 10–100 years [203]; thereafter, the star cools down in a quasistationary regime where the temperature distribution in the heat-insulating shell at each time instant unambiguously depends on the core temperature. We note that all currently observed neutron stars are at least several centuries old. This means that they are in the state of quasistationary cooling in the absence of fast energy release in the envelopes. The quasistationarity may be disturbed by the explosive thermonuclear burning of accreted matter [50] or the liberation of energy in the crust during starquakes [53–56].

Cooling in the quasistationary regime goes through the following stages [88]:

(1) The neutrino cooling stage lasts $\sim 10^5$ years. During this time, the core cools largely via neutrino emission in various physical reactions [30], the main ones being direct (if present) and modified Urca processes (depending on the particles involved), as well as neutrino bremsstrahlung radiation.

(2) The photon cooling (closing) stage begins at the stellar age of $t \gtrsim 10^5$ years when the lowered core temperature makes neutrino emission (strongly temperature-dependent) weaker than in cooling via heat transfer through the envelope and conversion into surface electromagnetic radiation.

The cooling curve of a neutron star depends on its mass M; the model of superdense matter in the core determining the equation of state (hence, the radius R) and composition of the core (hence, the intensity of neutrino emission at a given mass); and the envelope properties: (a) heat conductivity determining L_γ at a given core temperature, (b) neutrino luminosity in the crust, (c) sources of heating and their intensity. Characteristic thermal conductivity and neutrino luminosity of the envelopes at each time instant t (i.e., at the model-specific temperature T distribution in the envelopes), in turn, depend on the stellar mass M, the radius R, and the magnetic field (both magnetic induction B and the configuration of magnetic force lines may be essential).

Comparing the observed L_γ and t for neutron stars with the cooling curves allows estimating M and R and placing bounds on the theoretical models of superdense matter. This method for parameter evaluation is largely applicable to isolated neutron stars. By contrast, most neutron stars in binary systems have an additional source of energy (accretion) and an additional source of X-ray radiation (accretion disk), often much more powerful than L_γ.

7.2 Thermal structure

The complete set of equations describing the mechanical and thermal structure and evolution of a spherically symmetric star at hydrostatic equilibrium in the framework of GR was obtained by Thorne [202]. These equations are easy to transform to the form holding for the stellar envelope with radial heat transfer, a smooth temperature distribution over the surface, and a force-free magnetic field. Under the assumption that the heat transfer and neutrino emission are quasistationary, these equations reduce to a system of ordinary differential equations for the metric function Φ, local density of the radial heat flow F_r, temperature T, and gravitating mass m enclosed inside a sphere of a radius r as functions of the pressure P (see, e.g., [204]). The fitting factors of GR entering this system depend on the mass fraction $(M-m)/M$ outside the equipotential surface being considered and on the $P/\rho c^2$ ratio included in the TOV equation. At the outer–inner crust interface, $(M-m)/M \sim 10^{-5}$ and $P/\rho c^2 \sim 10^{-2}$; therefore, the GR correction factors are almost constant in the outer shells. Bearing this constancy in mind and disregarding the geometric thickness of the heat-insulating layer compared with R in the absence of heat sources and sinks in the thermoinsulating envelope of a neutron star, we obtain that the radial heat flow F_r through unit are is also constant and equals $\sigma_\mathrm{SB} T_\mathrm{s}^4$, where σ_SB is the Stefan–Boltzmann constant. Here and hereafter, we distinguish between the local surface temperature T_s and the integral effective temperature T_eff, because T_s may vary over the surface. Under the above conditions, calculating the thermal structure amounts to solving a simplified equation [205] written in a form coincident with the nonrelativistic equation $\kappa\,\mathrm{d}T/\mathrm{d}P = F_\mathrm{r}/\rho g$. Such an approximation is used in the majority of neutron star cooling research [88]. Magnetars have stronger magnetic fields and surface luminosities than ordinary neutron stars and have, in addition, internal sources of energy. This requires solving the complete set of equations taking neutrino emission rate per unit volume Q_v and heat source power Q_h into account, instead of the simplified heat transfer equation [100, 204].

The effective radial thermal conductivity at a local surface area in a magnetic field is $\kappa = \kappa_\parallel \cos^2\theta_\mathrm{B} + \kappa_\perp \sin^2\theta_\mathrm{B}$, where θ_B is the angle between magnetic force lines and the normal to the surface, and $\kappa_\parallel$ and $\kappa_\perp$ are components of the heat conductivity tensor responsible for the transfer along and across the force lines. In the heat-insulating envelope of a neutron star each of the components $\kappa_\parallel$ and $\kappa_\perp$ contains radiative κ_r and electron κ_e constituents. Photon heat conduction prevails ($\kappa_\mathrm{r} > \kappa_\mathrm{e}$) in the outermost (typically nondegenerate) layers, while electron heat conduction plays the main role in deeper, moderately or strongly degenerate layers. The total thermal flux along a given radius r (the local luminosity related to thermal but not neutrino losses) is defined by the flux density integral over the sphere of this radius, $L_r = \int \sin\theta\,\mathrm{d}\theta\,\mathrm{d}\varphi r^2 F_r(\theta,\varphi)$, where θ and φ are respectively the polar and azimuthal angles.

The use of equations holding for a spherically symmetric body at each point of the surface assumes that the mean radial temperature gradient is much greater than the lateral one. The estimates made in [204] indicate that this condition is fulfilled with a good accuracy at the largest part of the star surface, and corrections for deviations from a one-dimensional approximation make a negligibly small contribution to the total luminosity; this allows disregarding them in the first approximation.

In the quasistationary regime, the temperature of a neutron star increases monotonically from the external layers of the atmosphere to the interior of the envelope until it reaches equilibrium (usually in the outer crust). However, magnetars must have sources of heating in the envelopes capable of maintaining their high luminosity; for this reason, temperatures profiles in magnetar envelopes are nonmonotonic [100].

7.3 Cooling curves

The nonstationary problem is described by the same thermal balance equations [204], but the difference $Q = Q_\nu - Q_h$ is supplemented by the term $C\exp(-\Phi)\,\partial T/\partial t$, where C is the heat capacity per unit volume [203]. Strictly speaking, Q should be supplemented by another term describing the release of latent melting heat during the movement of the Coulomb fluid–crystal interface with a change in temperature. But this term is always neglected in the available programs for calculating the thermal evolution of neutron stars. Following the classic work [205], the nonstationary problem is solved in the interior of a neutron star where density surpasses a certain threshold value ρ_b; for external envelopes at $\rho < \rho_b$, whose relaxation time is small compared with characteristic times of thermal evolution, a stationary system of equations is solved. Traditionally, the value $\rho_b = 10^{10}$ g cm^{-3} is chosen in accordance with [205], but sometimes other ρ_b values prove more suitable, depending on the concrete problem of interest [100, 204, 206, 207]. The relation between the heat flow ρ_b across the boundary and the temperature T_b at this boundary obtained by solving the stationary problem for the envelopes serves as a boundary condition for the nonstationary problem in the internal region. It primarily depends on heat conductivity in the sensitivity strip on the $\rho - T$ plane close to the turning point at which $\kappa_e \sim \kappa_r$ [205]. Analytic estimates for the position of this point were obtained in [201].

The quantities T_s, T_{eff}, and L_γ are estimated with respect to the local reference frame at the surface of a neutron star. Quantities 'visible' for a distant observer must be corrected for the red shift (Section 2.1). The solution of the cooling problem is described in more detail in [203] (see also the references in [88, 208]).

The envelopes of a neutron star at birth consist of iron-group elements, which explains why calculations of cooling were for a long time made for iron-rich shells alone. However, the envelopes of a star that has passed through an accretion stage may consist of lighter elements. Accreted envelopes have a higher electron conductivity than iron-rich ones because more weakly charged ions scatter electrons less effectively. In other words, accretion makes the envelopes more transparent to the passing heat [209]. The core temperature at the neutrino cooling stage is regulated by neutrino emission and is practically independent of the properties of the envelopes; therefore, their transparency makes the star brighter due to an enhanced T_{eff}. At the later photon stage, the transparent envelopes more readily transmit heat and the star fades away faster. These effects are especially demonstrative when comparing the solid, dashed, and dotted curves in Fig. 7,[3] the difference between which is due to the different mass of accreted matter ΔM.

[3] The cooling curves presented in Figs 7 and 8 were calculated by D G Yakovlev for Ref. [210] using a relatively soft equation of state for which direct Urca processes are feasible at $M > 1.462 M_\odot$ (see [88]).

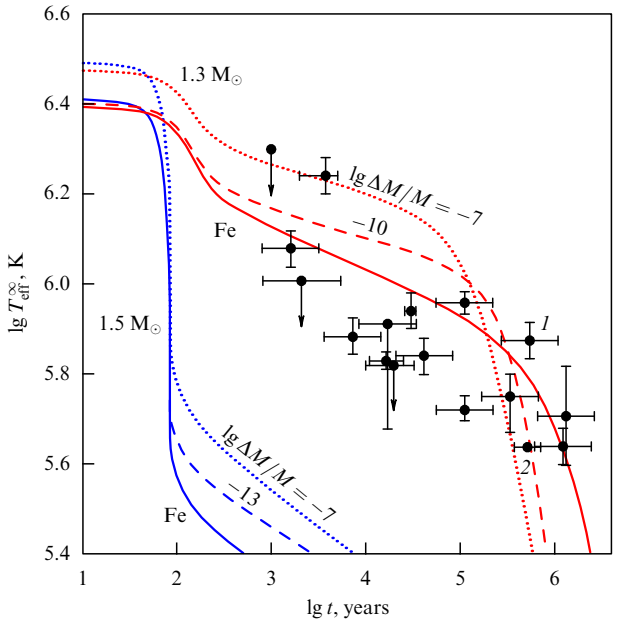

Figure 7. Cooling curves of neutron stars compared with some observation-based estimates of their temperatures and ages [208]. The cooling curves for different models of chemical composition of the heat-insulating envelope (in accordance with [206]) correspond to different accumulated masses ΔM of light elements: solid and dotted curves correspond to an iron envelope and an envelope of lighter nuclear composition, dashed curves correspond to a partly substituted envelope. The upper three curves correspond to a star with the mass $M = 1.3 M_\odot$ undergoing standard cooling by Murca processes and the lower three, to a star with the mass $M = 1.5 M_\odot$ undergoing enhanced cooling by direct Urca processes. Dots with error bars correspond to the published estimates of ages t and effective surface temperatures T_{eff}^{∞} of neutron stars; arrows pointing down indicate the upper bounds on T_{eff}^{∞}.

Similarly, cooling depends on a superstrong magnetic field. In a strong magnetic field where the electron cyclotron frequency ω_c exceeds the typical frequency of their collisions with plasma ions, heat transfer across magnetic field lines is hampered; therefore, those regions in which the lines are directed toward the surface become cooler. Oscillations of the heat conductivity coefficients (see Fig. 6) caused by Landau quantization facilitate heat transfer along magnetic field lines on an average, making the regions near the magnetic poles hotter. Taken together, enhanced luminosity near the poles and its reduction at the equator make integral luminosity of a star in a moderate magnetic field $B \lesssim 10^{13}$ G virtually the same as in the absence of a magnetic field. Although the temperature distribution over the surface depends on the field strength and configuration, the integral luminosity is virtually unrelated to B for both moderate dipole [206] and moderate small-scale [211] magnetic fields. A more substantial increase in the superstrong field $B \gtrsim 10^{14}$ G near the magnetic poles of magnetars is responsible for the effect of enhanced transparency of the envelopes, analogous to the effect of accretion, as shown in Fig. 8.

7.4 Effective temperatures

The upper and lower groups of three curves in Figs 7 and 8 correspond to standard and enhanced cooling. The latter occurs when direct Urca processes operate at the neutrino cooling stage in a star of a sufficiently large mass. The dots with error bars indicate estimated ages t and effective surface temperatures T_{eff}^{∞} obtained from observational data summar-

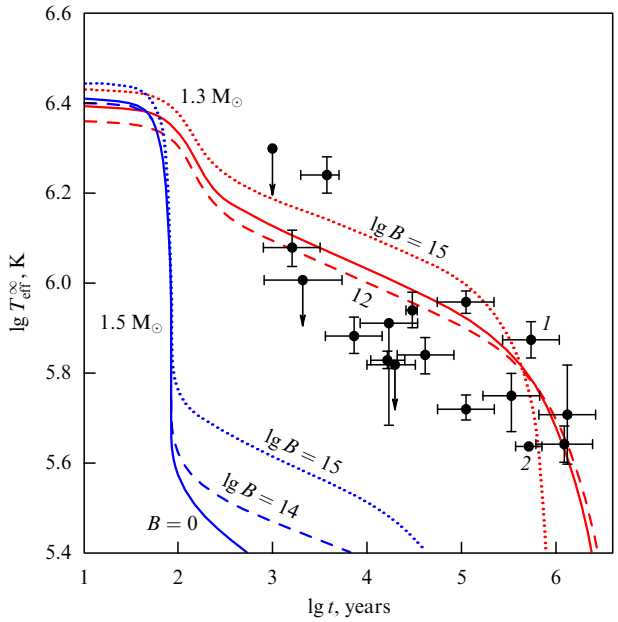

Figure 8. The same as in Fig. 7 for an iron envelope and different magnetic fields: solid and dotted curves correspond to $B = 0$ and 10^{15} Gs, dashed ones to an intermediate case.

ized in Ref. [208]. It follows from the figures that under favorable conditions, cooling curves give an idea of the stellar mass and properties of envelopes: the coldest stars of a given age appear to undergo enhanced cooling and are therefore massive, whereas the hottest ones have accreted envelopes.

Enhanced cooling may be a consequence not only of direct Urca processes in npeμ matter but also of analogous hyperon and quark Urca processes in exotic models of the inner core of a neutron star [125]. The rate of direct Urca processes is limited by a gap in the energy spectrum of superfluid nucleons [26]; therefore, nucleon superfluidity smooths the dependence of cooling curves on stellar mass, making the 'weighing' of the star by measuring its effective temperature more feasible [208]. Moreover, nucleon superfluidity, as well as hyperon and quark (color) superfluidity in exotic models, decreases the heat capacity of the stellar core [26], which also affects cooling.

In principle, therefore, comparison of measured ages and temperatures with cooling curves permits determining stellar mass and conjecturing the composition of the core and heat-insulating envelopes when the mass is known from independent estimates. But the results thus obtained should be interpreted with caution for the following reasons. Effective temperatures $T_{\rm eff}^{\infty}$ are typically measured by varying the parameters of a theoretical model used to calculate the emission spectrum. The parameters are chosen so as to most accurately reproduce the observed spectrum, but the final result strongly depends on the choice of the model. Certain estimates $T_{\rm eff}^{\infty}$ presented in Figs 7 and 8 were obtained using models of nonmagnetic and magnetic hydrogen atmospheres, while others simply assume that radiation is described by the Planck spectrum. For example, the fit to the three-component model spectrum was used for the thermal component of the PSR B1055–52 spectrum: the power-law component was added to two black-body components, whose cooling is believed to be responsible for heat radiation from the surface [212]. The result of this fitting is marked in the figures by the numeral 1, while the one marked by 2 was obtained for the radio-silent star RX J1856.4–3754 based on a physical model of the magnetic atmosphere [213] (see Section 7.5 for the details). For comparison, the authors of [213] fitted the observed X-ray spectrum of RX J1856.4–3745 to the Planck spectrum. The result of such simple fitting plotted in Figs 7 and 8 almost coincided with point *1*, meaning that the systematic error in the position of point *1* resulting from the absence of a model for the formation of the PSR B1055-52 spectrum may be of the same order as the distance between points *1* and *2*, that is, significantly greater than the statistical fitting error.

7.5 Masses and radii

Analysis of the thermal radiation spectrum of a neutron star provides information not only on its effective temperature but also on the radius and mass. We first consider the Planck spectrum disregarding intrastellar absorption and possible nonuniformity of the temperature distribution over the surface. $T_{\rm eff}^{\infty}$ is found from the position of the spectral maximum and the total (bolometric) flux of incoming radiation $F_{\rm bol}^{\infty}$ from its measured intensity. If a star is at a distance D from the observer, its photon luminosity is $L_{\gamma}^{\infty} = 4\pi D^2 F_{\rm bol}^{\infty}$. On the other hand, R_{∞} is found from $L_{\gamma}^{\infty} = 4\pi\sigma_{\rm SB} R_{\infty}^2 (T_{\rm eff}^{\infty})^4$ (in accordance with the Stefan–Boltzmann law).

The comparison of theoretical and measured spectra actually involves more unknown variables. The spectrum is distorted by absorption in the interstellar gas; therefore, spectral analysis can be used to determine average gas concentration over the line of sight. If the distance D is unknown, it can be estimated under the assumption of the typical concentration of the interstellar gas in a given galactic region, using D as a fitting parameter. The temperature distribution over the stellar surface may be nonuniform. For example, the thermal spectrum in the presence of hot polar caps consists of two Planck components, each having its own values $T_{\rm eff}^{\infty}$ and R_{∞}. Finally, because no star is an absolutely black body, the real radiation spectrum differs from the Planck spectrum. Spectrum simulation is a difficult task, involving solution of the equations of hydrostatic equilibrium, energy balance, and radiation transmission [214]. Coefficients of these equations depend on the chemical composition of the atmosphere, effective temperature, acceleration of gravity, and magnetic field. Different assumptions of the chemical composition, $T_{\rm eff}$, $z_{\rm g}$, and B values lead to different model spectra; their comparison with the observed spectrum permits obtaining acceptable parameter values. Knowing the shape of the spectrum, allows calculating the fitting coefficient by the Stefan–Boltzmann formula and finding R_{∞} from $F_{\rm bol}^{\infty}$. Simultaneous determination of $z_{\rm g}$ and $R_{\infty} = R(1 + z_{\rm g})$ allows the mass M to be computed by formulas (1) and (3).

We consider certain problems arising from the estimation of parameters of neutron stars from their observed thermal spectra using the 'Walter star' as an example (the nearby radio-silent star discovered in 1996 as a source of soft X-rays [90] and identified a year later in the optical range [205]). The first parallax measurement by the 'planetary camera' (PC) on board the Hubble space observatory gave the value $D \approx 60$ pc [216] corresponding to a very small radius R. This gave reason to believe that the object could be a quark star [217]. A reanalysis of the data yielded twice the previous distance, $D \approx 120$ pc [218], and independent treatment of the same data by different authors has led to $D \approx 140$ pc [219].

Finally, the measurement of parallax by the high resolution camera (HRC) of the same observatory yielded $D \approx 160$ pc [220]. Simultaneously, it was shown that the spectrum of the Walter star is not described by the black-body model: the fit of its X-ray region to the Planck spectrum predicts a much weaker luminosity in the optical range than the observed one. Attempts to describe the observed spectrum in terms of the models of atmospheres of different chemical compositions without a magnetic field and of the two-component Planck model are reported in [221] and [222]. It turned out that the hydrogen atmosphere model reproducing the X-ray spectral region predicts too high a luminosity in the optical range and models of atmospheres of a different chemical composition predict absorption lines unseen in observational studies. Fitting to the two-component model for the soft component of the composite spectrum leads to a bound on the radius $R_\infty > 17 \text{ km} \times (D/120 \text{ pc})$, which is difficult to relate to theoretical calculations of neutron star radii.

Simulation of the neutron star spectrum based on the solution of a system of equations for radiation transfer in a partly ionized hydrogen atmosphere of finite thickness above the condensed surface in a strong magnetic field was proposed in [213]. The authors used the atmosphere model in [162] based on the equation of state of the hydrogen plasma in a strong magnetic field and absorption/scattering coefficients in such a plasma presented in [95]. At $B \sim (3-4) \times 10^{12}$ G, $T_{\rm eff}^{\infty} = (4.34 \pm 0.03) \times 10^5$ K, $z_{\rm g} = 0.25 \pm 0.05$, and $R_\infty = 17.2^{+0.5}_{-0.1}\, d_{140}$ km, they managed for the first time to reproduce the measured spectrum of RX J1856.4–3745 in the X-ray to optical frequency range within the measurement errors of the best space and terrestrial observatories. The errors are given at the significance levels 1σ and $d_{140} \equiv D/(140 \text{ pc})$. It follows from these estimates, with account of expressions (1)–(3), that $R = 13.8^{+0.9}_{-0.6}\, d_{140}$ km and $M = 1.68^{+0.22}_{-0.15}\, d_{140}\, M_\odot$ for this neutron star. Disregarding the factor d_{140}, one might conclude that the 68% confidence interval lies above all the theoretical $R(M)$ dependences shown in Fig. 4. This would mean that either measurements or the theoretical model of the atmosphere is not quite accurate (setting aside a variant of the superstiff equation of state not shown in Fig. 4). The estimate of $D \approx 160$ pc [220] shifts the values of R and M even farther from the theoretical $R(M)$ dependence. Moreover, such a massive star should have undergone enhanced cooling, contrary to the data in Figs 7 and 8. At the same time, the earlier estimate $D \approx 120$ pc [218], recently confirmed in [111], removes all contradictions.

Therefore, the uncertainty of distance measurements proves more important than the inaccuracy of spectrum fitting. An even greater uncertainty is associated with the choice of a theoretical model. For example, fitting the X-ray region of the RX J1856.4–3745 spectrum with the black-body spectrum in [213] gave $R_\infty \approx 5\, d_{140}$ km.

Similar problems are encountered in the analysis of all known thermal spectra of isolated neutron stars. They are not infrequently supplemented by uncertainties of spectrum division into thermal and nonthermal components (see [89] and the references therein).

8. Conclusion

Neutron stars are miraculous objects in which Nature assembled its puzzles, whose solution is sought by seemingly unrelated branches of science, such as the physics of outer space and the micro-world, giant gravitating masses, and elementary particles. This makes neutron stars unique cosmic laboratories for the verification of basic physical concepts. In the last 50 years, both theoretical and observational studies of neutron stars have been developing at a progressively faster pace following advances in nuclear and particle physics on the one hand, and astronomy and experimental physics on the other hand.

The present review outlines some aspects of neutron star physics, describes methods for measuring their temperature, masses, and radii, and illustrates the relation between the theoretical interpretation of these data and the solution of fundamental physical problems.

The work was supported by the Russian Foundation for Basic Research (grant No. 08-02-00837) and the State Program for Support of Leading Scientific Schools of the Russian Federation (grant No. NSh-3769.2010.2).

Note added in proof

When this paper was being prepared for publication, P Demorest et al. reported the record-breaking mass $M = 1.97 \pm 0.04 M_\odot$ of the neutron star in the PSR J1614 2230 binary system (*Nature* **467** 1081, 2010). This estimate was obtained by measuring the Shapiro delay parameters (see Section 2.1 of the present review). Plotting it in our Fig. 4 results in the appearance of the corresponding vertical strip slightly to the left of point *2*. In conformity with the discussion in Section 4.4, it testifies to the inapplicability of superdense matter equations of state softer than SLy.

References

1. Fortov V E *Usp. Fiz. Nauk* **179** 653 (2009) [*Phys. Usp.* **52** 615 (2009)]
2. Glendenning N K *Compact Stars: Nuclear Physics, Particle Physics, and General Relativity* 2nd ed. (New York: Springer, 2000)
3. Shklovskii I S *Zvezdy: ikh Rozhdenie, Zhizn' i Smert'* (Stars: Their Birth, Life, and Death) (Moscow: Nauka, 1984) [Translated into English (San Francisco: W.H. Freeman, 1978)]
4. Ginzburg V L *Dokl. Akad. Nauk SSSR* **156** 43 (1964) [*Sov. Phys. Dokl.* **9** 329 (1964)]
5. Ginzburg V L, Ozernoi L M *Zh. Eksp. Teor. Fiz.* **47** 1030 (1964) [*Sov. Phys. JETP* **20** 689 (1965)]
6. Ginzburg V L, Kirzhnits D A *Zh. Eksp. Teor. Fiz.* **47** 2006 (1964) [*Sov. Phys. JETP* **20** 1346 (1965)]
7. Migdal A B *Zh. Eksp. Teor. Fiz.* **37** 249 (1959) [*Sov. Phys. JETP* **10** 176 (1960)]
8. Ginzburg V L *Usp. Fiz. Nauk* **97** 601 (1969) [*Sov. Phys. Usp.* **12** 241 (1969)]
9. Ginzburg V L, Syrovatskii *Dokl. Akad. Nauk SSSR* **158** 808 (1964) [*Sov. Phys. Dokl.* **9** 831 (1965)]
10. Ginzburg V L, Kirzhniz D A *Nature* **220** 148 (1968)
11. Ginzburg V L, Zheleznyakov V V, Zaitsev V V *Nature* **220** 355 (1968)
12. Ginzburg V L, Zaitsev V V *Nature* **222** 230 (1969)
13. Ginzburg V L, Zheleznyakov V V, Zaitsev V V *Usp. Fiz. Nauk* **98** 201 (1969); *Astrophys. Space Sci.* **4** 464 (1969)
14. Ginzburg V L, Zheleznyakov V V *Annu. Rev. Astron. Astrophys.* **13** 511 (1975)
15. Ginzburg V L, Zheleznyakov V V *Comm. Astrophys. Space Phys.* **2** 167 (1970)
16. Ginzburg V L, Zheleznyakov V V *Comm. Astrophys. Space Phys.* **2** 197 (1970)
17. Ginzburg V L *Highlights Astron.* **2** 737 (1971)
18. Ginzburg V L, Usov V V *Pis'ma Zh. Eksp. Teor. Fiz.* **15** 280 (1972) [*JETP Lett.* **15** 196 (1972)]
19. Ginzburg V L *Usp. Fiz. Nauk* **103** 393 (1971) [*Sov. Phys. Usp.* **14** 83 (1971)]; *Highlights Astron.* **2** 20 (1971)
20. ATNF Pulsar Catalogue, http://www.atnf.csiro.au/research/pulsar/psrcat/; Manchester R N et al. *Astron. J.* **129** 1993 (2005)
21. Bisnovatyi-Kogan G S *Usp. Fiz. Nauk* **176** 59 (2006) [*Phys. Usp.* **49** 53 (2006)]

22. Mereghetti S *Astron. Astrophys. Rev.* **15** 225 (2008)
23. Ginzburg V L *Rasprostranenie Elektromagnitnykh Voln v Plazme* (The Propagation of Electromagnetic Waves in Plasmas) 2nd ed. (Moscow: Nauka, 1967) [Translated into English (Oxford: Pergamon Press, 1970)]
24. Shapiro S L, Teukolsky S A *Black Holes, White Duarfs, and Neutron Stars*: *The Physics of Compact Objects* (New York: Wiley, 1983) [Translated into Russian (Moscow: Mir, 1985)]
25. Haensel P, Potekhin A Y, Yakovlev D G *Neutron Stars 1*: *Equation of State and Structure* (New York: Springer, 2007)
26. Yakovlev D G, Levenfish K P, Shibanov Yu A *Usp. Fiz. Nauk* **169** 825 (1999) [*Phys. Usp.* **42** 737 (1999)]
27. Beskin V S *Usp. Fiz. Nauk* **169** 1169 (1999) [*Phys. Usp.* **42** 1071 (1999)]
28. Malov I F *Radiopul'sary* (Radiopulsars) (Moscow: Nauka, 2004)
29. Michel F C *Adv. Space Res.* **33** 542 (2004)
30. Yakovlev D G et al. *Phys. Rep.* **354** 1 (2001)
31. Misner C W, Thorne K S, Wheeler J A *Gravitation* (San Francisco: W.H. Freeman, 1973) [Translated into Russian (Moscow: Mir, 1977)]
32. Tolman R C *Phys. Rev.* **55** 364 (1939)
33. Oppenheimer J R, Volkoff G M *Phys. Rev.* **55** 374 (1939)
34. Hessels J W T et al. *Science* **311** 1901 (2006)
35. Bonazzola S, Gourgoulhon E *Astron. Astrophys.* **312** 675 (1996)
36. Braginskii V B *Usp. Fiz. Nauk* **170** 743 (2000) [*Phys. Usp.* **43** 691 (2000)]
37. Popov S B, Prokhorov M E *Usp. Fiz. Nauk* **177** 1179 (2007) [*Phys. Usp.* **50** 1123 (2007)]
38. Kramer M, Stairs I H *Annu. Rev. Astron. Astrophys.* **46** 541 (2008)
39. Istomin Ya N *Pis'ma Astron. Zh.* **17** 711 (1991) [*Sov. Astron. Lett.* **17** 301 (1991)]
40. Kramer M *Astrophys. J.* **509** 856 (1998)
41. Champion D J et al. *Science* **320** 1309 (2008)
42. Freire P C C, arXiv:0907.3219
43. Shklovskii I S *Sverkhnovye Zvezdy i Svyazannye s Nimi Problemy* (Supernova Stars and Related Problems) 2nd ed. (Moscow: Nauka 1976) [Translated into English: *Supernovae* (New York: Wiley, 1968)]
44. Imshennik V S, Nadyozhin D K *Usp. Fiz. Nauk* **156** 561 (1988); in *Soviet Scientific Reviews, Ser. E*: *Astrophysics and Space Physics* Vol. 7 (Chur: Harwood Acad. Publ., 1989) p. 75
45. Imshennik V S *Space Sci. Rev.* **74** 325 (1995)
46. Arnett D *Supernovae and Nucleosynthesis* (Princeton: Princeton Univ. Press, 1996)
47. Woosley S, Janka H-T *Nature Phys.* **1** 147 (2005)
48. Paczyński È *Acta Astron.* **42** 145 (1992)
49. Postnov K A *Usp. Fiz. Nauk* **42** 469 (1999) [*Phys. Usp.* **42** 469 (1999)]
50. Strohmayer T, Bildsten L, in *Compact Stellar X-Ray Sources* (Eds W Lewin, M van der Klis) (Cambridge: Cambridge Univ. Press, 2006) p. 113
51. Ruderman M *Nature* **223** 597 (1969)
52. Baym G, Pines D *Ann. Physics* **66** 816 (1971)
53. Blaes O et al. *Astrophys. J.* **343** 839 (1989)
54. Haensel P, Denisov A, Popov S *Astron. Astrophys.* **240** 78 (1990)
55. Alpar M A *Adv. Space Res.* **21** 159 (1998)
56. Franco L M, Bennett L, Epstein R I *Astrophys. J.* **543** 987 (2000)
57. Reisenegger A et al. *Astrophys. J.* **653** 568 (2006)
58. Bisnovatyi-Kogan G S, Chechetkin V M *Usp. Fiz. Nauk* **127** 263 (1979) [*Sov. Phys. Usp.* **22** 89 (1979)]
59. Haensel P, Zdunik J L *Astron. Astrophys.* **227** 431 (1990)
60. Haensel P, Zdunik J L *Astron. Astrophys.* **404** L33 (2003)
61. Lipunov V M *Astropfizika Neitronnykh Zvezd* (Astrophysics of Neutron Stars) (Moscow: Nauka, 1987) [Translated into English (Berlin: Springer, 1992)]
62. Baade W, Zwicky F *Phys. Rev.* **45** 138 (1934)
63. Chadwick J *Nature* **129** 312 (1932)
64. Rosenfeld L, in *Astrophysics & Gravitation, Proc. 16th Solvay Conf. on Physics* (Brussels: Universite de Bruxelles, 1974) p. 174
65. Landau L D *Phys. Z. Sowjetunion* **1** 285 (1932)
66. Zwicky F *Astrophys. J.* **88** 522 (1938)
67. Cameron A G W *Astrophys. J.* **130** 916 (1959)
68. Bohr A, Mottelson È R, Pines D *Phys. Rev.* **110** 936 (1958)
69. Ambartsumyan V A, Saakyan G S *Astron. Zh.* **37** 193 (1960) [*Sov. Astron.* **4** 187 (1960)]
70. Zel'dovich Ya B *Zh. Eksp. Teor. Fiz.* **41** 1609 (1961) [*Sov. Phys. JETP* **14** 1143 (1962)]
71. Bahcall J N, Wolf R A *Phys. Rev.* **140** B1452 (1965)
72. Chiu H-Y, Salpeter E E *Phys. Rev. Lett.* **12** 413 (1964)
73. Stabler R C, Ph.D. Thesis (Ithaca, NY: Cornell Univ., 1960)
74. Morton D C *Nature* **201** 1308 (1964)
75. Bahcall J N, Wolf R A *Astrophys. J.* **142** 1254 (1965)
76. Tsuruta S, Cameron A G W *Can. J. Phys.* **44** 1863 (1966)
77. Pacini F *Nature* **216** 567 (1967)
78. Giacconi R et al. *Phys. Rev. Lett.* **9** 439 (1962)
79. Becker W, Trümper J *Astron. Astrophys.* **326** 682 (1997)
80. Zeldovich Ya B, Guseynov H *Astrophys. J.* **144** 840 (1966)
81. Kardashev N S *Astron. Zh.* **4** 1807 (1964) [*Sov. Astron.* **8** 643 (1965)]
82. Hewish A et al. *Nature* **217** 709 (1968)
83. Hewish A *Rev. Mod. Phys.* **47** 567 (1975)
84. Gold T *Nature* **218** 731 (1968)
85. Shklovsky I S *Astrophys. J.* **148** L1 (1967)
86. de Freitas Pacheco J A, Steiner J E, Neto A D *Astron. Astrophys.* **55** 111 (1977)
87. Cameron A G W, Mock M *Nature* **215** 464 (1967)
88. Yakovlev D G, Pethick C J *Annu. Rev. Astron. Astrophys.* **42** 169 (2004)
89. Zavlin V E, in *Neutron Stars and Pulsars* (Ed. W Becker) (New York: Springer, 2009) p. 181
90. Walter F M, Wolk S J, Neuhäuser R *Nature* **379** 233 (1996)
91. de Luca A *AIP Conf. Proc.* **983** 311 (2008)
92. Haberl F *Astrophys. Space Sci.* **308** 181 (2007)
93. Halpern J P, Gotthelf E V *Astrophys. J.* **709** 436 (2010)
94. Popov S B, Prokhorov M E *Astrofizika Odinochnykh Neitronnykh Zvezd*: *Radiotikhie Neitronnye Zvezdy i Magnitary* (Astrophysics of Isolated Neutron Stars: Radio-Silent Neutron Stars and Magnetars) (Moscow: GAISh MGU, 2002)
95. Potekhin A Y, Chabrier G *Astrophys. J.* **585** 955 (2003)
96. Potekhin A Y *Astron. Astrophys.* **518** A24 (2010)
97. Thompson C, in *The Neutron Star — Black Hole Connection* (Eds C Kouveliotou, J Ventura, E Van den Heuvel) (Dordrecht: Kluwer Acad. Publ., 2001) p. 369
98. Urpin V, Konenkov D *Astron. Astrophys.* **483** 223 (2008)
99. Pons J A, Miralles J A, Geppert U *Astron. Astrophys.* **496** 207 (2009)
100. Kaminker A D et al. *Mon. Not. R. Astron. Soc.* **395** 2257 (2009)
101. Manchester R N, Taylor J M *Pulsars* (San Francisco: W.H. Freeman, 1977) [Translated into Russian (Moscow: Mir, 1980)]
102. Stephenson F R, Green D A *Historical Supernovae and their Remnants* (Oxford: Oxford Univ. Press, 2002)
103. Zavlin V E *Astrophys. Space Sci.* **308** 297 (2007)
104. Malov I F, Machabeli G Z *Anomal'nye Pul'sary* (Anomalous Pulsars) (Moscow: Nauka, 2009)
105. Ertan Ü et al. *Astrophys. Space Sci.* **308** 73 (2007)
106. van der Klis M et al. *Nature* **316** 225 (1985)
107. van der Klis M *Annu. Rev. Astron. Astrophys.* **38** 717 (2000)
108. Kluzniak M et al. *Rev. Mex. Astron. Astrophys.* **27** 18 (2007)
109. Tagger M *Rev. Mex. Astron. Astrophys.* **27** 26 (2007)
110. Shaposhnikov N, Titarchuk L *Astrophys. J.* **606** L57 (2004)
111. Steiner A W, Lattimer J M, Brown E F *Astrophys. J.* **722** 33 (2010)
112. Brown E F, Bildsten L, Rutledge R E *Astrophys. J.* **504** L95 (1998)
113. Brown E F, Cumming A *Astrophys. J.* **698** 1020 (2009)
114. Shternin P S et al. *Mon. Not. R. Astron. Soc.* **382** L43 (2007)
115. Akmal A, Pandharipande V R, Ravenhall D G *Phys. Rev. C* **58** 1804 (1998)
116. Douchin F, Haensel P *Astron. Astrophys.* **380** 151 (2001)
117. Pandharipande V R, Ravenhall D G, in *Nuclear Matter and Heavy Ion Collisions* (Eds M Soyeur et al.) (Dordrecht: D. Reidel, 1989) p. 103
118. Douchin F, Haensel P *Phys. Lett. B* **485** 107 (2000)
119. Heiselberg H, Hjorth-Jensen M *Phys. Rep.* **328** 237 (2000)
120. Haensel P, Potekhin A Y *Astron. Astrophys.* **428** 191 (2004)
121. Bocquet M et al. *Astron. Astrophys.* **301** 757 (1995)
122. Walecka J D *Ann. Physics* **83** 491 (1974)
123. Gamow G, Schoenberg M *Phys. Rev.* **59** 539 (1941)
124. Gamov G *My World Line*: *An Informal Autobiography* (New York: Viking Press, 1970) [Translated into Russian (Moscow: Nauka, 1994)]
125. Haensel P *Space Sci. Rev.* **74** 427 (1995)
126. Salpeter E E *Ann. Physics* **11** 393 (1960)

127. Balberg S, Gal A *Nucl. Phys. A* **625** 435 (1997)
128. Migdal A B *Zh. Eksp. Teor. Fiz.* **61** 2209 (1971) [*Sov. Phys. JETP* **34** 1184 (1972)]
129. Sawyer R F *Phys. Rev. Lett.* **29** 382 (1972); *Phys. Rev. Lett.* **29** 823 (1972), erratum
130. Scalapino D J *Phys. Rev. Lett.* **29** 386 (1972)
131. Migdal A B *Usp. Fiz. Nauk* **123** 369 (1977) [*Sov. Phys. Usp.* **20** 879 (1977)]
132. Kunihiro T, Takatsuka T, Tamagaki R *Prog. Theor. Phys. Suppl.* **112** 197 (1993)
133. Kaplan D B, Nelson A E *Phys. Lett. B* **175** 57 (1986)
134. Ramos A, Schaffner-Bielich J, Wambach J *Lecture Notes Phys.* **578** 175 (2001)
135. Kolomeitsev E E, Voskresensky D N *Phys. Rev. C* **68** 015803 (2003)
136. Glendenning N K, Schaffner-Bielich J *Phys. Rev. Lett.* **81** 4564 (1998)
137. Dremin I M, Kaidalov A B *Usp. Fiz. Nauk* **176** 275 (2006) [*Phys. Usp.* **49** 263 (2006)]
138. Ivanenko D D, Kurdgelaidze D F *Astrofizika* **1** 479 (1965) [*Astrophysics* **1** 251 (1965)]
139. Collins J C, Perry M J *Phys. Rev. Lett.* **34** 1353 (1975)
140. Kurkela A, Romatschke P, Vuorinen A *Phys. Rev. D* **81** 105021 (2010)
141. Blaschke D et al. *Phys. Rev. C* **80** 065807 (2009)
142. Iosilevskiy I *Acta Phys. Polon. B Proc. Suppl.* **3** 589 (2010)
143. Glendenning N K *Phys. Rev. D* **46** 1274 (1992)
144. Cazzola P, Lucaroni L, Scarinci C *Nuovo Cimento B* **43** 250 (1966)
145. Takemori M T, Guyer R A *Phys. Rev. D* **11** 2696 (1975)
146. Pandharipande V R, Smith R A *Phys. Lett. B* **59** 15 (1975)
147. Takatsuka T, Tamagaki R *Prog. Theor. Phys.* **58** 694 (1977)
148. Kutschera M, Wójcik W *Phys. Lett. B* **223** 11 (1989)
149. Takatsuka T, Tamagaki R *Prog. Theor. Phys.* **79** 274 (1988)
150. Kristian J et al. *Nature* **338** 234 (1989)
151. Kristian J *Nature* **349** 747 (1991)
152. Pethick C J, Ravenhall D G *Annu. Rev. Nucl. Part. Sci.* **45** 429 (1995)
153. Chugunov A I, Haensel P *Mon. Not. R. Astron. Soc.* **381** 1143 (2007)
154. Aguilera D N et al. *Phys. Rev. Lett.* **102** 091101 (2009)
155. Pethick C J, Potekhin A Y *Phys. Lett. B* **427** 7 (1998)
156. Ravenhall D G, Pethick C J, Wilson J R *Phys. Rev. Lett.* **50** 2066 (1983)
157. Lorenz C P, Ravenhall D G, Pethick C J *Phys. Rev. Lett.* **70** 379 (1993)
158. Gusakov M E et al. *Astron. Astrophys.* **421** 1143 (2004)
159. Potekhin A Y, Chabrier G *Phys. Rev. E* **62** 8554 (2000)
160. Lai D *Rev. Mod. Phys.* **73** 629 (2001)
161. Baiko D A et al. *Phys. Rev. Lett.* **81** 5556 (1998)
162. Potekhin A Y et al. *Astrophys. J.* **612** 1034 (2004)
163. Ho W C G, Potekhin A Y, Chabrier G *Astrophys. J. Suppl. Ser.* **178** 102 (2008)
164. Mori K, Ho W C G *Mon. Not. R. Astron. Soc.* **377** 905 (2007)
165. Dall'Osso S, Shore S N, Stella L *Mon. Not. R. Astron. Soc.* **398** 1869 (2009)
166. Chandrasekhar S, Fermi E *Astrophys. J.* **118** 116 (1953)
167. Lai D, Shapiro E E *Astrophys. J.* **383** 745 (1991)
168. Reisenegger A, in *Proc. of the Intern. Workshop on Strong Magnetic Fields and Neutron Stars* (Eds H J Mosquera Cuesta, H Perez Rojas, C A Zen Vasconcellos) (La Habana, Cuba: ICIMAF, 2003) p. 33
169. Bisnovatyi-Kogan G S *Astrophys. Space Sci.* **189** 147 (1992)
170. Thompson C, Duncan R C *Astrophys. J.* **408** 194 (1993)
171. Baym G, Pethick C, Pines D *Nature* **224** 674 (1969)
172. Cumming A, Arras P, Zweibel E *Astrophys. J.* **609** 999 (2004)
173. Landau L D *Z. Phys.* **64** 629 (1930)
174. Pavlov G G, Gnedin Yu N *Sov. Sci. Rev. E Astrophys. Space Phys.* **3** 197 (1984)
175. Ho W C G, Lai D *Mon. Not. R. Astron. Soc.* **338** 233 (2003)
176. Trümper J et al. *Astrophys. J.* **219** L105 (1978)
177. Enoto T et al. *Publ. Astron. Soc. Jpn.* **60** S57 (2008)
178. Rodes-Roca J J et al. *Astron. Astrophys.* **508** 395 (2009)
179. Santangelo A et al. *Astrophys. J.* **523** L85 (1999)
180. Bignami G F et al. *Nature* **423** 725 (2003)
181. Suleimanov V F, Pavlov G G, Werner K *Astrophys. J.* **714** 630 (2010)
182. Broderick A, Prakash M, Lattimer J M *Astrophys. J.* **537** 351 (2000)
183. Johnson È R, Hirschfelder J O, Yang K-H *Rev. Mod. Phys.* **55** 109 (1983)
184. Ruder H et al. *Atoms in Strong Magnetic Fields*: *Quantum Mechanical Treatment and Applications in Astrophysics and Quantum Chaos* (Berlin: Springer, 1994)
185. Ruderman M A *Phys. Rev. Lett.* **27** 1306 (1971)
186. Potekhin A Y *J. Phys. B At. Mol. Opt. Phys.* **31** 49 (1998)
187. Detmer T, Schmelcher P, Cederbaum L S *Phys. Rev. A* **57** 1767 (1998)
188. Kappes U, Schmelcher P *Phys. Rev. A* **53** 3869 (1996)
189. Turbiner A V *Astrophys. Space Sci.* **308** 267 (2007)
190. Medin Z, Lai D *Phys. Rev. A* **74** 062508 (2006)
191. Burkova L A et al. *Zh. Eksp. Teor. Fiz.* **71** 526 (1976) [*Sov. Phys. JETP* **44** 276 (1976)]
192. Ipatova I P, Maslov A Yu, Subashiev A V *Zh. Eksp. Teor. Fiz.* **87** 1804 (1984) [*Sov. Phys. JETP* **60** 1037 (1984)]
193. Vincke M, Le Dourneuf M, Baye D *J. Phys. B At. Mol. Opt. Phys.* **25** 2787 (1992)
194. Potekhin A Y *J. Phys. B At. Mol. Opt. Phys.* **27** 1073 (1994)
195. Bezchastnov V G, Pavlov G G, Ventura J *Phys. Rev. A* **58** 180 (1998)
196. Pavlov G G, Bezchastnov V G *Astrophys. J.* **635** L61 (2005)
197. Vincke M, Baye D *J. Phys. B At. Mol. Opt. Phys.* **21** 2407 (1988)
198. Pavlov G G, Mészáros P *Astrophys. J.* **416** 752 (1993)
199. Yakovlev D G, Kaminker A D, in *The Equation of State in Astrophysics* (Eds G Chabrier, E Schatzman) (Cambridge: Cambridge Univ. Press, 1994) p. 214
200. Potekhin A Y *Astron. Astrophys.* **351** 787 (1999)
201. Ventura J, Potekhin A, in *The Neutron Star — Black Hole Connection* (Eds C Kouveliotou, J Ventura, E Van den Heuvel) (Dordrecht: Kluwer Acad. Publ., 2001) p. 393
202. Thorne K S *Astrophys. J.* **212** 825 (1977)
203. Gnedin Y, Yakovlev D G, Potekhin A Y *Mon. Not. R. Astron. Soc.* **324** 725 (2001)
204. Potekhin A Y, Chabrier G, Yakovlev D G *Astrophys. Space Sci.* **308** 353 (2007); astro-ph/0611014, corrected version v3
205. Gudmundsson E H, Pethick C J, Epstein R I *Astrophys. J.* **272** 286 (1983)
206. Potekhin A Y et al. *Astrophys. J.* **594** 404 (2003)
207. Yakovlev D G et al. *Astron. Astrophys.* **417** 169 (2004)
208. Yakovlev D G et al. *AIP Conf. Proc.* **983** 379 (2008)
209. Potekhin A Y, Chabrier G, Yakovlev D G *Astron. Astrophys.* **323** 415 (1997)
210. Chabrier G, Saumon D, Potekhin A Y *J. Phys. A*: *Math. Gen.* **39** 4411 (2006)
211. Potekhin A Y, Urpin V, Chabrier G *Astron. Astrophys.* **443** 1025 (2005)
212. Pavlov G G, Zavlin V E, in *Texas in Tuscany. XXI Symp. on Relativistic Astrophysics, Florence, Italy, 9–13 December 2002* (Eds. R Bandiera, R Maiolino, F Mannucci) (Singapore: World Scientific, 2003) p. 319
213. Ho W C G et al. *Mon. Not. R. Astron. Soc.* **375** 821 (2007)
214. Mihalas D *Stellar Atmospheres* 2nd ed. (San Francisco: W.H. Freeman, 1978) [Translated into Russian (Moscow: Mir, 1982)]
215. Walter F M, Matthews L D *Nature* **389** 358 (1997)
216. Walter F M *Astrophys. J.* **549** 433 (2001)
217. Drake J J et al. *Astrophys. J.* **572** 996 (2002)
218. Walter F M, Lattimer J M *Astrophys. J.* **576** L145 (2002)
219. Kaplan D L, van Kerkwijk M H, Anderson J *Astrophys. J.* **571** 447 (2002)
220. van Kerkwijk M H, Kaplan D L *Astrophys. Space Sci.* **308** 191 (2007)
221. Pons J A et al. *Astrophys. J.* **564** 981 (2002)
222. Burwitz V et al. *Astron. Astrophys.* **399** 1109 (2003)